

# **Report on the relationship of early-life stressors with fetal and childhood brain developmental outcomes and the extent to which these mediate associations of early-life exposures with mental health and psychopathology life course trajectories**

LifeCycle report D6.3

## Authors:

Hanan El Marroun (ERASMUS)

Marieke Welten (ERASMUS)

Jordi Julvez (ISGLOBAL)

Jordi Sunyer (ISGLOBAL)

Version 2.0

Delivery date: Month 66

### **Document Information**

Grant Agreement No.	<b>733206</b>
Project Title	Early-life stressors and LifeCycle health (The LifeCycle Project)
Project Start Date	01 January 2017
Work package title	WP6 - Early-life stressors and mental health life course trajectories
Related task(s)	Task 6.3 - Identify early brain development that mediates the relationships between early-life stressors and later mental health and disease.
Lead Organisation	Erasmus MC
Submission date	19 September 2022
Dissemination Level	Public

## Table of Contents

List of Figures.....	3
List of Abbreviations .....	4
Executive summary .....	6
1. Introduction.....	7
2. Neuroimaging Protocol .....	7
3. Main contain Project Results .....	8
3.1 Urban exposures (air pollution) and brain development.....	8
3.2 Radiofrequency electromagnetic fields and brain development.....	11
3.3 Child risk factors and brain development .....	13
3.4 Prenatal risk factors and brain development .....	17
4. Conclusion .....	26
5. Contribution of partners .....	26
6. Deviations from original plan .....	27
7. Dissemination activities .....	27
8. References .....	28
Appendix 1.....	30

## List of Figures

*Figure 1:* Differences in cortical thickness at 6–10 years of age associated with air pollution exposure during fetal life

*Figure 2:* Brain regions identified on the adjusted associations between exposure to OC, PM<sub>2.5</sub>abs, and Cu during pregnancy and cortical thickness (mm), OP<sub>DTT</sub>, and UFP during childhood and cortical thickness (mm), and Zn, OP<sub>ESR</sub>, and PM<sub>COARSE</sub> and cortical surface area (mm<sup>2</sup>) at 9–12 years of age.

*Figure 3:* Median daily RF dose (mJ/kg/day) in brain regions and whole-body

*Figure 4:* Associations Between Polygenic Scores for Psychiatric Disorders and Cognition and Brain Volumes

*Figure 5:* T1-weighted MRI scan (axial, sagittal and coronal view) showing the amygdala and hippocampus segmentation.

*Figure 6:* The association of adolescent alcohol use and cortical brain volumes (main and interaction effects) in the BrainScale, BrainTime and the Generation R Study.

*Figure 7:* Gestational Age at Birth and Cortical Thickness, Surface Area, and Gyrfication in All Children.

*Figure 8:* Maternal depressive symptoms at child age 2 months and child cortical thickness at age 10 in a population-based study of maternal depressive symptoms and offspring brain development.

*Figure 9:* White matter tracts associated with maternal BMI.

*Figure 10:* The white matter tracts of global fractional anisotropy (FA) and global mean diffusivity (MD) that are associated with <18 weeks, 18-25 weeks, and averaged: maternal dimethyl (DM) and diethyl (DE) alkyl phosphate metabolite concentrations in nmol/g creatinine.

*Figure 11:* 25(OH)D status from mid-gestation to delivery in relation to surface-based cortical metrics in children at 10 years

## List of Abbreviations

25(OH)D: 25-hydroxyvitamin D  
3D: 3-dimensional  
A: Anterior  
ADHD: attention-deficit/hyperactivity disorder  
ASD: autism spectrum disorder  
BMI: body mass index  
CI: Confidence Interval  
CGC: Cingulum bundle  
CST: corticospinal tract  
Cu: elemental copper  
DAP: dialkylphosphates  
DataSHaPER: DataSchema and Harmonization Platform for Epidemiological Research;  
<http://www.datashaper.org>  
DE: diethyl  
DECT: digital enhanced communication technology  
DM: dimethyl  
DSA: Deletion/Substitution/Addition  
DTI: Diffusion Tensor Imaging  
ENIGMA: Enhancing Neuroimaging Genetics Through Meta-analysis  
<http://enigma.ini.usc.edu>  
FA: fractional anisotropy  
FDR: false discovery rate  
FMI: forceps minor  
GAB: Gestational Age at Birth  
GM: Gray matter  
I: Inferior  
ILF: inferior longitudinal fasciculus  
INMA: Infancia y Media Ambiente  
K: elemental potassium  
L: Lateral  
LC-PUFA: long-chain polyunsaturated fatty acids  
LH: Left Hemisphere  
M: Medial  
MeDALL: Mechanisms of the Development of Allergy  
MD: mean diffusivity  
MRI: Magnetic Resonance Imaging  
NFBC1986/1966: Northern Finland Birth Cohorts  
NOX: nitrogen oxides  
OC: organic carbon  
OP: organophosphate  
P: Posterior  
PGSs: polygenic scores  
PM: particulate matter with different aerodynamic diameters: between 10  $\mu\text{m}$  and 2.5  $\mu\text{m}$  ( $\text{PM}_{\text{COARSE}}$ ), and less than 2.5  $\mu\text{m}$  ( $\text{PM}_{2.5}$ )  
 $\text{PM}_{2.5\text{abs}}$ : absorbance of  $\text{PM}_{2.5}$  filters  
PUFAs: polyunsaturated fatty acids

RF: radiofrequency electromagnetic fields  
RF-EMF: radiofrequency electromagnetic fields  
RH: Right Hemisphere  
S: Superior  
SDS: Standard Deviation Score)  
SLF: superior longitudinal fasciculus  
UFP: ultra-fine particles  
UNC: uncinated fasciculus  
WM: White Matter  
Zn: elemental zinc

## Executive summary

The aim of Task 6.3 in the LifeCycle project is to report on the relationship of early life stressors with fetal and childhood brain developmental outcomes and the extent to which these mediate associations of early life exposures with mental health and psychopathology life course trajectories. Stressors in this context include those introduced through socio-economic, migration, urban environment, and lifestyle factors. This report describes fundamental work undertaken in the development of mental health trajectories in the LifeCycle project and presents overviews and findings from our analysis for each step of this work. This includes a comprehensive harmonization protocol for cohorts participating in task 6.3 in the LifeCycle project that have neuroimaging data available. This harmonization has been completed to facilitate parallel and meta-analyses of data in the LifeCycle cohorts across neuroimaging domains. In addition, results from analyses about early life stressors and brain development, as well as the mediating role of brain development on behavioral or cognitive outcomes are presented here. Collectively, the results show that early factors in pregnancy and childhood may affect brain development, and that these differences in brain morphology may mediate child cognitive and behavioral outcomes. Finally, dissemination activities around task 6.3 are presented. Dissemination activities included several media outlets and presentations at scientific conferences. Future studies should investigate how these stressors interact and affect brain development and focus on mechanistic studies. On the long-term increased understanding on how early life stressors affect child development can be improve clinical practice and inform policy.



## 1. Introduction

The general aim of task 6.3 in the LifeCycle project was to study brain development from the fetal period and childhood onwards by means of advanced imaging studies including repeated fetal ultrasound and childhood MRI brain studies. These imaging data will be both structural and functional, and include for example total brain volume, hippocampal volume and functional connectivity. The measures were used to assess the role of brain developmental adaptations that may mediate the relationships between early-life stressors and later mental health and disease. We will identify stressors and critical periods in early life underlying the brain developmental adaptations that may lead to later life dysfunction and disease. We will first study the role of brain developmental adaptations in fetal life or childhood (Generation R, INMA, ALSPAC, BIB, NFBC1986, RAINE) and subsequently try to replicate the findings in adults (NFBC1966). The output of this task will provide insights to the role of developmental structural and functional brain developmental adaptations in the relationships between early-life stressors and mental health trajectories.

## 2. Neuroimaging Protocol

Traditionally, most neuroimaging studies have been limited to analyses on single-center datasets to minimize instrument-related variability in the data. However, in recent years there is an increasing trend towards data sharing in neuroimaging research communities, with multiple collaborative efforts for pooling existing data resources to form large, diverse samples covering a wide age range (Alfaro-Almagro et al 2019; Thompson et al. 2014). Such collective efforts are critical for enabling development of diagnostic and prognostic biomarkers that apply across different imaging equipment as well as across the broad spectrum of demographics, which is essential for translation of neuroimaging research into clinical settings.

To enable pooled analyses and meta-analyses in the future a harmonization protocol for the neuroimaging measures was developed. The aim of this specific neuroimaging protocol is to guide the cohorts in the harmonization process to generate variables that will be comparable across cohorts and measurements. The harmonization strategy was based on an adaptation of the DataSHaPER guidelines aimed to facilitate a rigorous, transparent and effective harmonization, made in the framework of the MeDALL project, like in the complete work package (WP 6), as well as neuroimaging networks that are existing (e.g., ENIGMA, <http://enigma.ini.usc.edu>). The neuroimaging protocol can be found in **Appendix 1**.

### 3. Main contain Project Results

Within task 6.3 several papers investigating early life exposures with brain morphology outcomes or using the brain measures as mediators have been published. Below an overview of the finalized projects.

#### 3.1 Urban exposures (air pollution) and brain development

##### Project 1: Air Pollution Exposure During Fetal Life, Brain Morphology, and Cognitive Function in School-Age Children (1)

**Involved partners:** ISGLOBAL, ERASMUS

Air pollution exposure during fetal life has been related to impaired child neurodevelopment, but it is unclear if brain structural alterations underlie this association. The authors assessed whether air pollution exposure during fetal life alters brain morphology and whether these alterations mediate the association between air pollution exposure during fetal life and cognitive function in school-age children.

We used data from a population-based birth cohort set up in Rotterdam, The Netherlands (2002–2006). Residential levels of air pollution during the entire fetal period were calculated using land-use regression models. Structural neuroimaging and cognitive function were performed at 6 to 10 years of age ( $n = 783$ ). Models were adjusted for several socioeconomic and lifestyle characteristics.

Mean fine particle levels were  $20.2 \mu\text{g}/\text{m}^3$  (range,  $16.8\text{--}28.1 \mu\text{g}/\text{m}^3$ ). Children exposed to higher particulate matter levels during fetal life had thinner cortex in several brain regions of both hemispheres (e.g., cerebral cortex of the precuneus region in the right hemisphere was  $0.045 \text{ mm}$  thinner (95% confidence interval,  $0.028\text{--}0.062$ ) for each  $5\text{-}\mu\text{g}/\text{m}^3$  increase in fine particles). The reduced cerebral cortex in precuneus and rostral middle frontal regions partially mediated the association between exposure to fine particles and impaired inhibitory control (see **Figure 1** below). Air pollution exposure was not associated with global brain volumes.

Exposure to fine particles during fetal life was related to child brain structural alterations of the cerebral cortex, and these alterations partially mediated the association between exposure to fine particles during fetal life and impaired child inhibitory control. Such cognitive impairment at early ages could have significant long-term consequences.



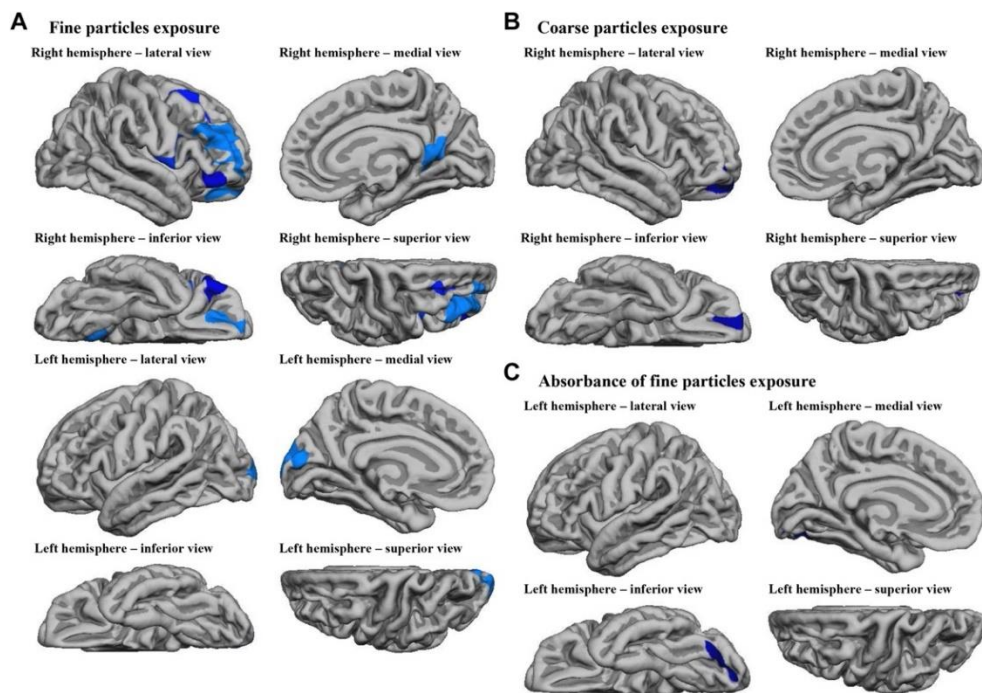


**Figure 1. Differences in cortical thickness at 6–10 years of age associated with air pollution exposure during fetal life:** (A) fine particles exposure, (B) coarse particles exposure, and (C) absorbance of fine particles exposure. The colored regions on the surface map represent brain regions that are thinner in relation to higher exposure to air pollution during fetal life in the right and left hemisphere (darker color indicates stronger association). Analyses were adjusted for child's gender and age. All brain regions survived the correction (Monte Carlo null-Z simulation with 10,000 iterations) for multiple comparisons ( $p < .01$ ).

## Project 2: Air pollution exposure – during pregnancy and childhood and brain morphology in preadolescents (2)

### **Involved partners:** ERASMUS & ISGLOBAL

Studies investigating the relationship between exposure to air pollution and brain development using magnetic resonance images are emerging. However, most studies have focused only on prenatal exposures, and have included a limited selection of pollutants. Here, we aim to expand the current knowledge by studying pregnancy and childhood exposure to a wide selection of pollutants, and brain morphology in preadolescents. We used data from 3133 preadolescents from a birth cohort from Rotterdam, the Netherlands (enrollment: 2002–2006). Concentrations of nitrogen oxides, coarse, fine, and ultrafine particles, and composition of fine particles were estimated for participant's home addresses in pregnancy and childhood, using land use regression models. Structural brain images were obtained at age 9–12 years. We assessed the relationships of air pollution exposure, with brain volumes, and surface-based morphometric data, adjusting for socioeconomic and life-style characteristics, using single as well as multi-pollutant approach.

No associations were observed between air pollution exposures and global volumes of total brain, and cortical and subcortical grey matter. However, we found associations between higher pregnancy and childhood air pollution exposures with smaller corpus callosum, smaller hippocampus, larger amygdala, smaller nucleus accumbens, and larger cerebellum (e.g., -69.2mm<sup>3</sup> hippocampal volume [95%CI -129.1 to -9.3] per 1ng/m<sup>3</sup> increase in pregnancy exposure to polycyclic aromatic hydrocarbons). Higher pregnancy exposure to air pollution was associated with smaller cortical thickness while higher childhood exposure was associated with predominantly larger cortical surface area. Higher pregnancy or childhood exposure to several air pollutants was associated with altered volume of several brain structures, as well as with cortical thickness and surface area (**Figure 2**). Associations showed some similarity to delayed maturation and effects of early-life stress.

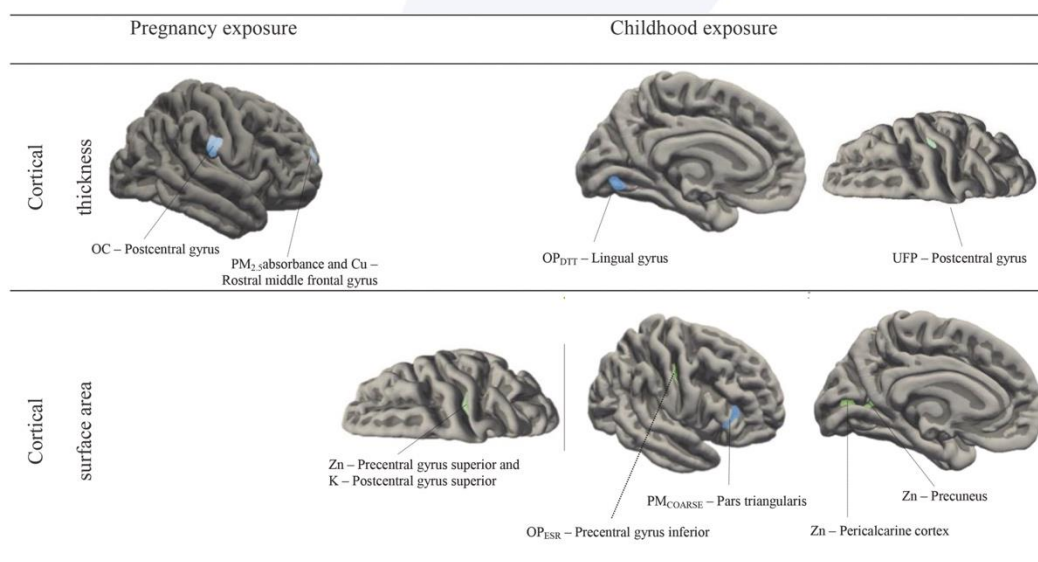


**Figure 2. Brain regions identified on the adjusted associations between exposure to OC, PM<sub>2.5</sub>abs, and Cu during pregnancy and cortical thickness (mm), OP<sub>DTT</sub>, and UFP during childhood and cortical thickness (mm), and Zn, OP<sub>ESR</sub>, and PM<sub>COARSE</sub> and cortical surface area (mm<sup>2</sup>) at 9–12 years of age.**  
Abbreviations: Cu, elemental copper; K, elemental potassium; OC, organic carbon; PM, particulate matter with different aerodynamic diameters: between 10 μm and 2.5 μm (PM<sub>COARSE</sub>), and less than 2.5 μm (PM<sub>2.5</sub>); PM<sub>2.5</sub>abs, absorbance of PM<sub>2.5</sub> filters; UFP, ultra-fine particles; Zn, elemental zinc.

### Project 3: Exposure to Air Pollution during Pregnancy and Childhood, and White Matter Microstructure in Preadolescents (3)

**Involved partners:** ERASMUS, ISGLOBAL

Air pollution has been related to brain structural alterations, but a relationship with white matter microstructure is unclear.

We assessed whether pregnancy and childhood exposures to air pollution are related to white matter microstructure in preadolescents.

We used data of 2,954 children from the Generation R Study, a population-based birth cohort from Rotterdam, Netherlands (2002–2006). Concentrations of 17 air pollutants including nitrogen oxides (NOX) particulate matter (PM), and components of PM were estimated at participants' homes during pregnancy and childhood using land-use regression models. Diffusion tensor images were obtained at child's 9–12 years of age, and fractional anisotropy (FA) and mean diffusivity (MD) were computed. We performed linear regressions adjusting for socioeconomic and lifestyle characteristics. Single-pollutant analyses were followed by multipollutant analyses using the Deletion/Substitution/Addition (DSA) algorithm.

In the single-pollutant analyses, higher concentrations of several air pollutants during pregnancy or childhood were associated with significantly lower FA or higher MD ( $p < 0.05$ ). In multipollutant models of pregnancy exposures selected by DSA, higher concentration of fine particles was associated with significantly lower FA [ $-0.71$  (95% CI:  $-1.26, -0.16$ ) per  $5 \mu\text{g}/\text{m}^3$  fine particles] and higher concentration of elemental silicon with significantly higher MD [ $0.06$  (95% CI:  $0.01, 0.11$ ) per  $100 \text{ ng}/\text{m}^3$  silicon]. Multipollutant models of childhood exposures selected by DSA indicated significant associations of NOX with FA [ $-0.14$  (95% CI:  $-0.23, -0.04$ ) per  $20\text{-}\mu\text{g}/\text{m}^3$  NOX increase], and of elemental zinc and the oxidative potential of PM with MD [ $0.03$  (95% CI:  $0.01, 0.04$ ) per  $10\text{-ng}/\text{m}^3$  zinc increase and  $0.07$  (95% CI:  $0.00, 0.44$ ) per  $1\text{-nmol DTT}/\text{min}/\text{m}^3$  oxidative potential increase]. Mutually adjusted models of significant exposures during pregnancy and childhood indicated significant associations of silicon during pregnancy, and zinc during childhood, with MD. Exposure in pregnancy and childhood to air pollutants from tailpipe and non-tailpipe emissions were associated with lower FA and higher MD in white matter of preadolescents.

## 3.2 Radiofrequency electromagnetic fields and brain development

### Project 1: Radiofrequency electromagnetic fields from mobile communication: Description of modeled dose in brain regions and the body in European children and adolescents (4)

**Involved partners:** ERASMUS & ISGLOBAL

Little is known about radiofrequency electromagnetic fields (RF) from mobile technology and resulting dose in young people. We describe modeled integrated RF dose in European children and adolescents combining own mobile device use and surrounding sources.

Using an integrated RF model, we estimated the daily RF dose in the brain (whole-brain, cerebellum, frontal lobe, midbrain, occipital lobe, parietal lobe, temporal lobes) and the whole-body in 8358 children (ages 8–12) and adolescents (ages 14–18) from the Netherlands, Spain, and Switzerland during 2012–2016. The integrated model estimated RF



dose from near-field sources (digital enhanced communication technology (DECT) phone, mobile phone, tablet, and laptop) and far-field sources (mobile phone base stations via 3D-radiowave modeling or RF measurements).

Adolescents were more frequent mobile phone users and experienced higher modeled RF doses in the whole-brain (median 330.4 mJ/kg/day) compared to children (median 81.8 mJ/kg/day). Children spent more time using tablets or laptops compared to adolescents, resulting in higher RF doses in the whole-body (median whole-body dose of 81.8 mJ/kg/day) compared to adolescents (41.9 mJ/kg/day). Among brain regions, temporal lobes received the highest RF dose (medians of 274.9 and 1786.5 mJ/kg/day in children and adolescents, respectively) followed by the frontal lobe. In most children and adolescents, calling on 2G networks was the main contributor to RF dose in the whole-brain (medians of 31.1 and 273.7 mJ/kg/day, respectively). These results are displayed in **Figure 3**. This first large study of RF dose to the brain and body of children and adolescents shows that mobile phone calls on 2G networks are the main determinants of brain dose, especially in temporal and frontal lobes, whereas whole-body doses were mostly determined by tablet and laptop use. The modeling of RF doses provides valuable input to epidemiological research and to potential risk management regarding RF exposure in young people.

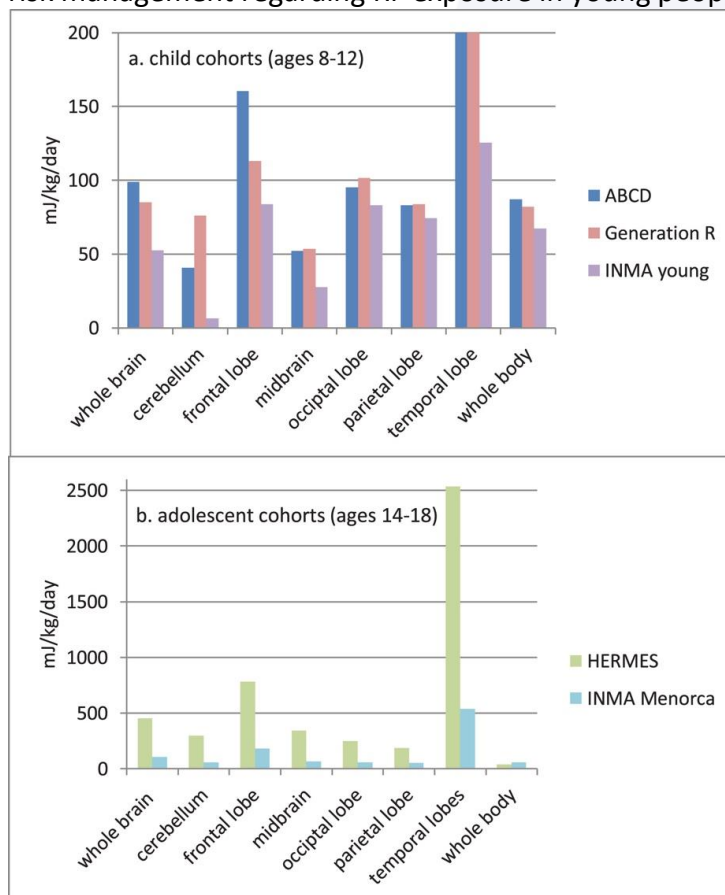


**Figure 3. Median daily RF dose (mJ/kg/day) in brain regions and whole-body.** By cohort among a) child cohorts (smaller scale) and b) adolescent cohorts (larger scale).

## Project 2: Estimated whole-brain and lobe-specific radiofrequency electromagnetic fields doses and brain volumes in preadolescents (5)

**Involved partners:** ERASMUS, ISGLOBAL

The objective was to assess the association between estimated whole-brain and lobe-specific radiofrequency electromagnetic fields (RF-EMF) doses, using an improved integrated RF-EMF exposure model, and brain volumes in preadolescents at 9–12 years old. Cross-sectional analysis in preadolescents aged 9–12 years from the Generation R Study, a population-based birth cohort set up in Rotterdam, The Netherlands (n = 2592). An integrated exposure model was used to estimate whole-brain and lobe-specific RF-EMF doses (mJ/kg/day) from different RF-EMF sources including mobile and Digital Enhanced Cordless Telecommunications (DECT) phone calls, other mobile phone uses than calling, tablet use, laptop use, and far-field sources. Whole-brain and lobe-specific RF-EMF doses were estimated for all RF-EMF sources together (i.e. overall) and for three groups of RF-EMF sources that lead to a different pattern of RF-EMF exposure. Information on brain volumes was extracted from magnetic resonance imaging scans.

Estimated overall whole-brain RF-EMF dose was 84.3 mJ/kg/day. The highest overall lobe-specific dose was estimated in the temporal lobe (307.1 mJ/kg/day). Whole-brain and lobe-specific RF-EMF doses from all RF-EMF sources together, from mobile and DECT phone calls, and from far-field sources were not associated with global, cortical, or subcortical brain volumes. However, a higher whole-brain RF-EMF dose from mobile phone use for internet browsing, e-mailing, and text messaging, tablet use, and laptop use while wirelessly connected to the internet was associated with a smaller caudate volume.

Our results suggest that estimated whole-brain and lobe-specific RF-EMF doses were not related to brain volumes in preadolescents at 9–12 years old. Screen activities with mobile communication devices while wirelessly connected to the internet lead to low RF-EMF dose to the brain and our observed association may thus rather reflect effects of social or individual factors related to these specific uses of mobile communication devices. However, we cannot discard residual confounding, chance finding, or reverse causality. Further studies on mobile communication devices and their potential negative associations with brain development are warranted, regardless whether associations are due to RF-EMF exposure or to other factors related to their use.

### 3.3 Child risk factors and brain development

## Project 1: Common Polygenic Variations for Psychiatric Disorders and Cognition in Relation to Brain Morphology in the General Pediatric Population (6)

**Involved partners:** ISGLOBAL, ERASMUS

This study examined the relation between polygenic scores (PGSs) for 5 major psychiatric disorders and 2 cognitive traits with brain magnetic resonance imaging morphologic measurements in a large population-based sample of children. In addition, this study tested for differences in brain morphology-mediated associations between PGSs for psychiatric disorders and PGSs for related behavioral phenotypes.

Participants included 1,139 children from the Generation R Study assessed at 10 years of age with genotype and neuroimaging data available. PGSs were calculated for



schizophrenia, bipolar disorder, major depression disorder, attention-deficit/hyperactivity disorder (ADHD), autism spectrum disorder, intelligence, and educational attainment using results from the most recent genome-wide association studies. Image processing was performed using FreeSurfer to extract cortical and subcortical brain volumes. Greater genetic susceptibility for ADHD was associated with smaller caudate volume (strongest prior = 0.01:  $\beta = -0.07$ ,  $p = .006$ ). In boys, mediation analysis estimates showed that 11% of the association between the PGS for ADHD and the PGS attention problems was mediated by differences in caudate volume ( $n = 535$ ), whereas mediation was not significant in girls or the entire sample. PGSs for educational attainment and intelligence showed positive associations with total brain volume (strongest prior = 0.5:  $\beta = 0.14$ ,  $p = 7.12 \times 10^{-8}$ ; and  $\beta = 0.12$ ,  $p = 6.87 \times 10^{-7}$ , respectively). These results are also shown in **Figure 4**. The present findings indicate that the neurobiological manifestation of polygenic susceptibility for ADHD, educational attainment, and intelligence involve early morphologic differences in caudate and total brain volumes in childhood. Furthermore, the genetic risk for ADHD might influence attention problems through the caudate nucleus in boys.

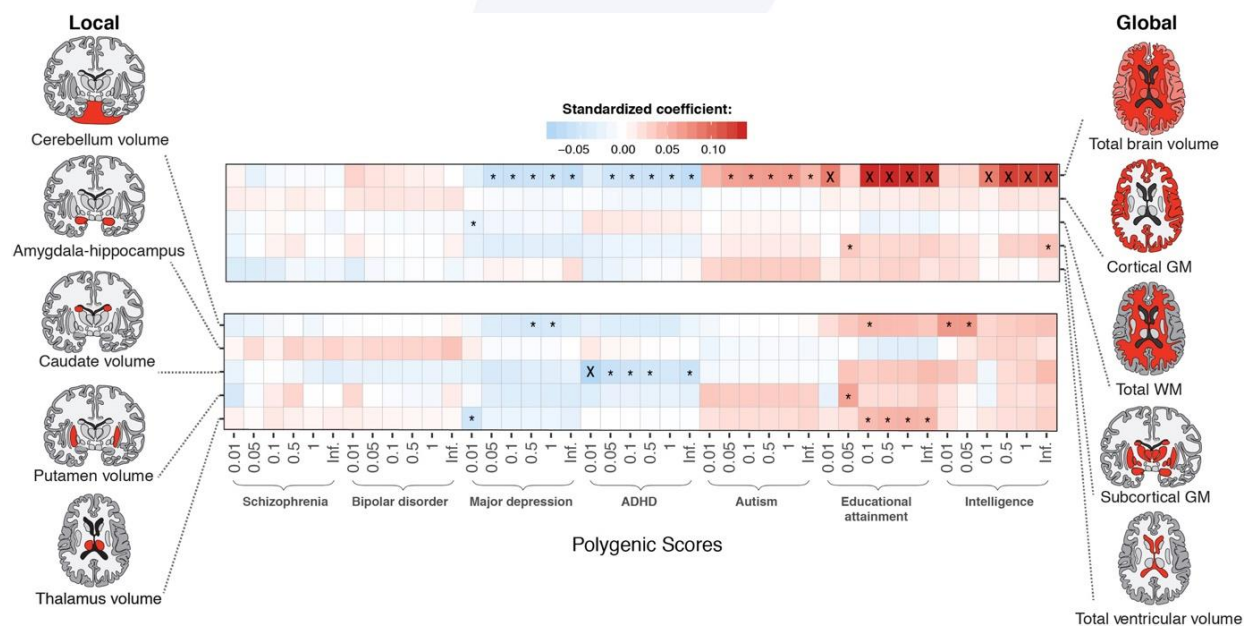


**Figure 4. Associations Between Polygenic Scores for Psychiatric Disorders and Cognition and Brain Volumes (N = 1,139).** All associations were adjusted for sex, age, total intracranial volume (except associations with total brain volume) and the first 4 genetic components. Uncorrected p values less than .05 (\*) and p values less than .05 by false discovery rate correction (X) are presented. ADHD = attention-deficit/hyperactivity disorder; GM = gray matter; WM = white matter.

**Project 2: Observed infant-parent attachment and brain morphology in middle childhood— A population-based study (7)**

**Involved partners:** ERASMUS

Poor quality of the early infant-parent bond predicts later child problems. Infant-parent attachment has been suggested to influence brain development, but this association has hardly been examined. In adults, larger amygdala volumes have been described in relation

to early attachment disorganization; neuroimaging studies of attachment in children, however, are lacking.

We examined the association between infant-parent attachment and brain morphology in 551 children from a population-based cohort in the Netherlands. Infant-parent attachment was observed with the Strange-Situation Procedure at age 14 months and different brain measures were collected with magnetic resonance imaging at mean age 10 years. Main outcomes were the hippocampus and amygdala (**Figure 5**). Children with disorganized infant attachment had larger hippocampal volumes than those with organized attachment patterns. This finding was robust to the adjustment for confounders and consistent across hemispheres. The association was not explained by cognitive or emotional and behavioral problems. Disorganized attachment did not predict any other difference in brain morphology. Moreover, children with insecure organized infant attachment patterns did not differ from those who were securely attached in any brain outcome.

Causality cannot be inferred, but our findings in this large population-based study provide novel evidence for a long-term association between the quality of infant-parent attachment and specific brain differences in childhood.

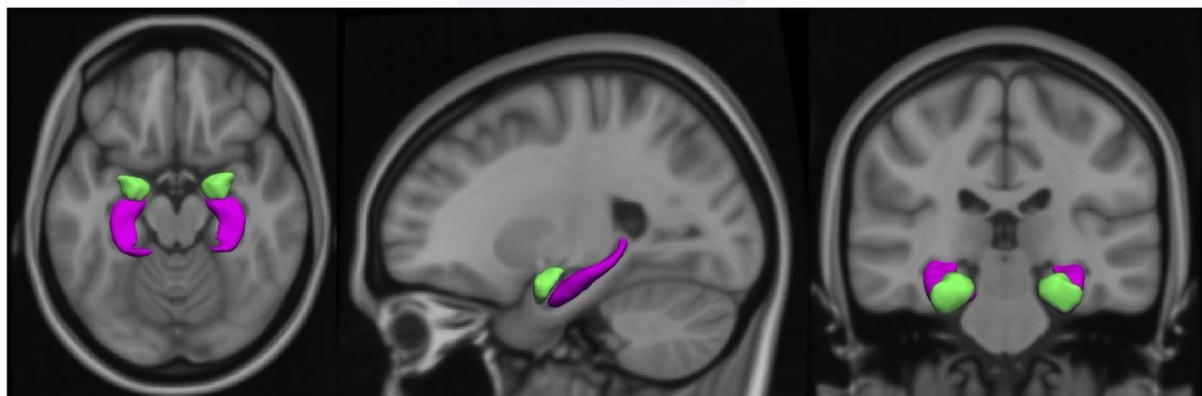


**Figure 5.** T1-weighted MRI scan (axial, sagittal and coronal view) showing the amygdala (in green) and hippocampus (in purple) segmentation.

### Project 3: Body fat, cardiovascular risk factors and brain structure in school-age children (8)

**Involved partners:** ERASMUS

In adults, cardiovascular risk factors are known to be associated with brain health. We hypothesized that these associations are already present at school-age. We examined the associations of adverse body fat measures and cardiovascular risk factors with brain structure, including volumetric measures and white matter microstructure, in 10-year-old children.

We performed a cross-sectional analysis in a population-based prospective cohort study in Rotterdam, the Netherlands. Analyses were based on 3098 children aged 10 years with neuroimaging data and at least one measurement of body fat and cardiovascular risk factors. Body fat measures included body mass index (BMI), fat mass index and android fat mass percentage obtained by Dual-energy X-ray absorptiometry. Cardiovascular risk factors included blood pressure, and serum glucose, insulin and lipids blood concentrations.

Structural neuroimaging, including global and regional brain volumes, was quantified by magnetic resonance imaging. DTI was used to assess white matter microstructure, including global fractional anisotropy (FA) and mean diffusivity (MD).

As compared to children with a normal weight, those with underweight had a smaller total brain and white matter volumes (differences  $-18.10$  (95% Confidence Interval (CI)  $-30.97, -5.22$ )  $\text{cm}^3$ ,  $-10.64$  (95% CI  $-16.82, -4.47$ )  $\text{cm}^3$ , respectively). In contrast, one SDS (Standard Deviation Score) increase in fat mass index was associated with a smaller gray matter volume (differences  $-3.48$  (95% CI  $-16.82, -4.47$ )  $\text{cm}^3$ ). Also, one SDS increase in android fat mass percentage was associated with lower white matter diffusivity (difference  $-0.06$  (95% CI  $-0.10, -0.02$ ) SDS). None of the other cardiovascular risk factors were associated with any of the brain outcomes. Body fat measures, but not other cardiovascular risk factors, were associated with structural neuroimaging outcomes in school-aged children. Prospective studies are needed to assess causality, direction and long-term consequences of the associations.

#### Project 4: Alcohol use and brain morphology in adolescence: A longitudinal study in three different cohorts (9)

##### **Involved partners:** ERASMUS

Alcohol consumption is commonly initiated during adolescence, but the effects on human brain development remain unknown. In this multisite study, we investigated the longitudinal associations of adolescent alcohol use and brain morphology. Three longitudinal cohorts in the Netherlands (BrainScale  $n = 200$ , BrainTime  $n = 239$  and a subsample of the Generation R study  $n = 318$ ) of typically developing participants aged between 8 and 29 years were included. Adolescent alcohol use was self-reported. Longitudinal neuroimaging data were collected for at least two time points. Processing pipelines and statistical analyses were harmonized across cohorts. Main outcomes were global and regional brain volumes, which were a priori selected. Linear mixed effect models were used to test main effects of alcohol use and interaction effects of alcohol use with age in each cohort separately. Alcohol use was associated with adolescent's brain morphology showing accelerated decrease in grey matter volumes, in particular in the frontal and cingulate cortex volumes, and decelerated increase in white matter volumes (**Figure 6**). No dose–response association was observed. The findings were most prominent and consistent in the older cohorts (BrainScale and BrainTime). In summary, this longitudinal study demonstrated differences in neurodevelopmental trajectories of grey and white matter volume in adolescents who consume alcohol compared with non-users. These findings highlight the importance to further understand underlying neurobiological mechanisms when adolescents initiate alcohol consumption. Therefore, further studies need to determine to what extent this reflects the causal nature of this association, as this longitudinal observational study does not allow for causal inference.



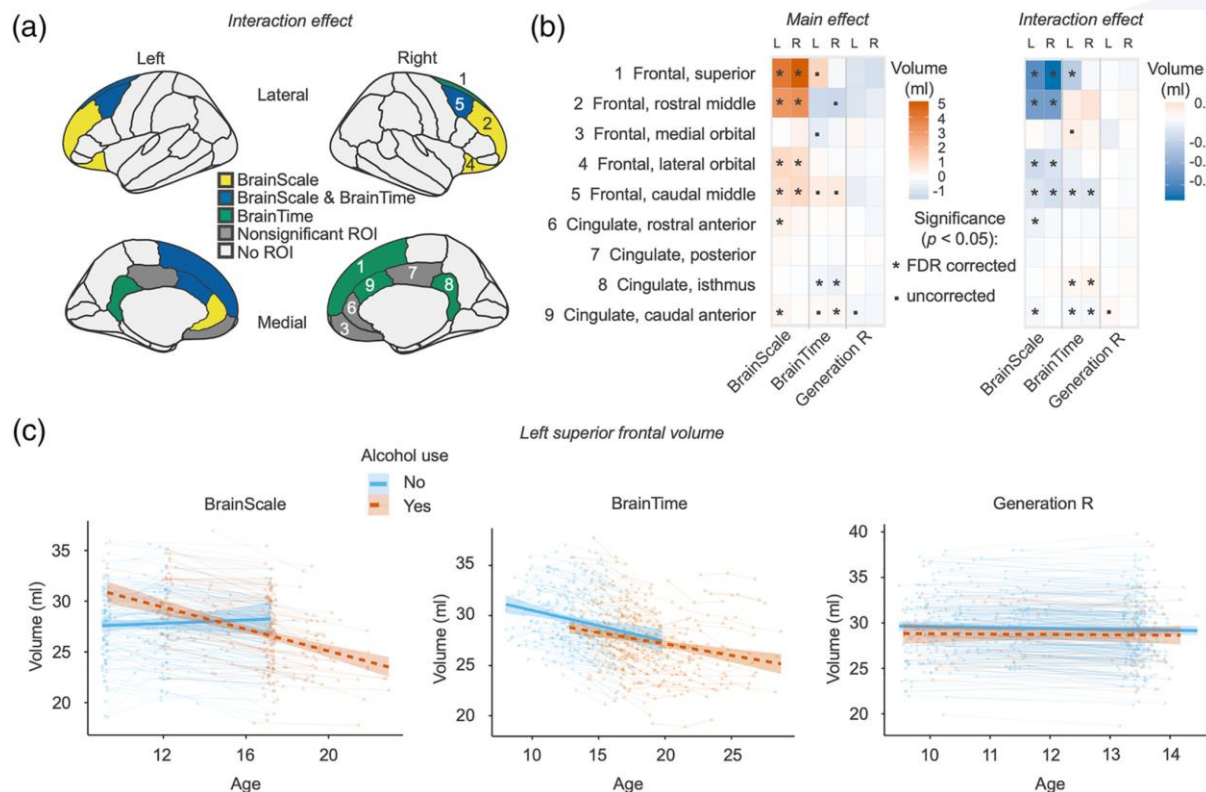


**Figure 6. The association of adolescent alcohol use and cortical brain volumes (main and interaction effects) in the BrainScale, BrainTime and the Generation R Study.** All volumes were converted from mm<sup>3</sup> to ml. Panel (a) shows the cortical brain regions that were found to be associated with the interaction effects in the three cohorts. Panel (b) shows the direction of the associations of adolescent alcohol use and cortical brain volumes found in the three cohorts in two correlograms (one for the main effects and one for the interaction effects). Panel (c) shows the individual subject data for the left superior frontal volume in each cohort (never drinking vs. ever drinking). FDR, false discovery rate

### 3.4 Prenatal risk factors and brain development

#### Project 1: Association of Gestational Age at Birth With Brain Morphometry (10)

**Involved partners:** ERASMUS

Preterm and postterm births are associated with adverse neuropsychiatric outcomes. However, it remains unclear whether variation of gestational age within the 37- to 42-week range of term deliveries is associated with neurodevelopment.

The aim was to investigate the association of gestational age at birth (GAB) with structural brain morphometry in children aged 10 years.

This population-based cohort study included pregnant women living in Rotterdam, the Netherlands, with an expected delivery date between April 1, 2002, and January 31, 2006.

The study evaluated 3079 singleton children with GAB ranging from 26.3 to 43.3 weeks and structural neuroimaging at 10 years of age from the Generation R Study, a longitudinal, population-based prospective birth cohort from early pregnancy onward in Rotterdam. Data

analysis was performed from March 1, 2019, to February 28, 2020, and at the time of the revision based on reviewer suggestions.

GAB was calculated based on ultrasonographic assessment of crown-rump length (<12 weeks 5 days) or biparietal diameter ( $\geq 12$  weeks 5 days) in dedicated research centers. As main outcomes brain structure, including global and regional brain volumes and surface-based cortical measures (thickness, surface area, and gyrification), was quantified by magnetic resonance imaging.

In the 3079 children (1546 [50.2%] female) evaluated at 10 years of age, GAB was linearly associated with global and regional brain volumes. Longer gestational duration was associated with larger brain volumes; for example, every 1-week-longer gestational duration corresponded to an additional 4.5 cm<sup>3</sup>/wk. (95% CI, 2.7-6.3 cm<sup>3</sup>/wk.) larger total brain volume. These associations persisted when the sample was restricted to children born at term (GAB of 37-42 weeks: 4.8 cm<sup>3</sup>/wk.; 95% CI, 1.8-7.7 cm<sup>3</sup>/wk.). GAB was related to surface area differences and gyrification as well (see **Figure 7**), but not with cortical thickness. No evidence of nonlinear associations between GAB and brain morphometry was observed.

In this cohort study, gestational duration was linearly associated with brain morphometry during childhood, including within the window of term delivery. These findings may have marked clinical importance, particularly given the prevalence of elective cesarean deliveries.



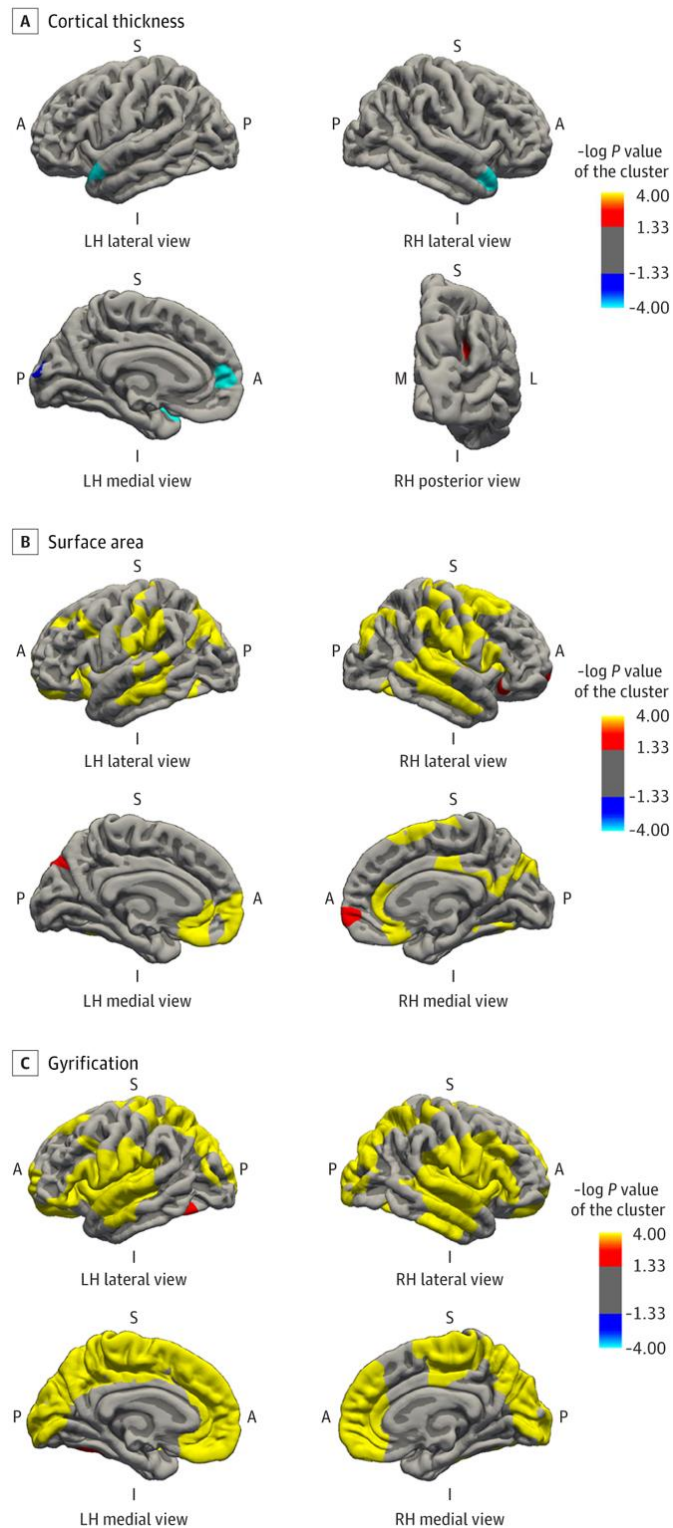


**Figure 7. Gestational Age at Birth and Cortical Thickness, Surface Area, and Gyrification in All Children.** Surface-based analysis was performed for 3065 children with a gestational age at birth ranging from 26.3 to 43.4 weeks. The model was adjusted for child sex, child age at neuroimaging, maternal ethnicity, maternal age at intake, marital status, educational level, psychopathologic conditions during pregnancy, smoking and alcohol use during pregnancy, and family income. Colored clusters represent regions of the brain that were positively (red to yellow) and negatively (dark to light blue) associated with gestational age at birth that survived the cluster wise (Monte Carlo simulation with 5000 iterations) correction for multiple comparisons ( $P < .001$ ). A indicates anterior; I, inferior; L, lateral; LH, left hemisphere; M, medial; P, posterior; RH, right hemisphere; S, superior.

## Project 2: Patterns of Fetal and Infant Growth and Brain Morphology at Age 10 Years (11)

**Involved partners:** ERASMUS

Preterm birth and low birth weight are associated with brain developmental and neurocognitive outcomes in childhood; however, not much is known about the specific critical periods in fetal life and infancy for these outcomes. The objective was to examine the associations of fetal and infant growth patterns with brain morphology in children at school age.

This population-based, prospective cohort study was conducted from February 1 to April 16, 2021, as a part of the Generation R Study in Rotterdam, the Netherlands. The study included 3098 singleton children born between April 1, 2002, and January 31, 2006.

Fetal weight was estimated in the second and third trimesters of pregnancy by ultrasonography. Infant weight was measured at birth and at 6, 12, and 24 months. Fetal and infant weight acceleration or deceleration were defined as a change in SD scores greater than 0.67 between time points. Infant measurements also included peak weight velocity, and age and body mass index reached at adiposity peak.

Brain structure, including global and regional brain volumes, was quantified by magnetic resonance imaging at age 10 years.

The study evaluated 3098 children (mean [SD] age at follow-up, 10.1 [0.6] years; 1557 girls [50.3%]; and 1753 Dutch [57.8%]). One SD score–higher weight gain until the second and third trimesters, birth, and 6, 12, and 24 months was associated with larger total brain volume independently of growth during any other age windows (second trimester: 5.7 cm<sup>3</sup>; 95% CI, 1.2-10.2 cm<sup>3</sup>; third trimester: 15.3 cm<sup>3</sup>; 95% CI, 11.0-19.6 cm<sup>3</sup>; birth: 20.8 cm<sup>3</sup>; 95% CI, 16.4-25.1 cm<sup>3</sup>; 6 months: 15.6 cm<sup>3</sup>; 95% CI, 11.2-19.9 cm<sup>3</sup>; 12 months: 11.3 cm<sup>3</sup>; 95% CI, 7.0-15.6 cm<sup>3</sup>; and 24 months: 11.1 cm<sup>3</sup>; 95% CI, 6.8-15.4 cm<sup>3</sup>). Compared with children with normal fetal and infant growth, those with fetal and infant growth deceleration had the smallest total brain volume (–32.5 cm<sup>3</sup>; 95% CI, –53.2 to –11.9 cm<sup>3</sup>). Children with fetal weight deceleration followed by infant catch-up growth had similar brain volumes as children with normal growth. Higher peak weight velocity and body mass index reached at adiposity peak were associated with larger brain volumes. Similar results were observed for cerebral and cerebellar gray and white matter volumes.

This cohort study's findings suggest that both fetal and infant weight growth might be critical for cerebral and cerebellar brain volumes during childhood. Whether these associations link to neurocognitive outcomes should be further studied.

## Project 3: Exposure to Maternal Depressive Symptoms in Fetal Life or Childhood and Offspring Brain Development: A Population-Based Imaging Study (12)

**Involved partners:** ERASMUS

The authors examined associations of exposure to maternal depressive symptoms at different developmental stages from fetal life to preadolescence with child brain development, including volumetrics and white matter microstructure.

This study was embedded in a longitudinal birth cohort in Rotterdam, the Netherlands.

Participants were 3,469 mother-child pairs with data on maternal depressive symptoms and child neuroimaging at age 10. The authors also measured child emotional and behavioral problems at the time of neuroimaging. The association of maternal depressive symptoms

with child brain development at each assessment was examined. Maternal depressive symptom trajectories were modeled across fetal life and childhood to determine the association of maternal depressive symptom patterns over time with child brain development.

The single-time-point analyses showed that maternal depressive symptoms at child age 2 months were associated with smaller total gray matter volume and lower global fractional anisotropy (FA), whereas maternal depressive symptoms assessed prenatally or in childhood were not. The trajectory analyses suggested in particular that children exposed to persistently high levels of maternal depressive symptoms across the perinatal period had smaller gray and white matter volumes as well as alterations (i.e., lower FA) in white matter microstructure compared with nonexposed children. Furthermore, the gray matter volume differences mediated the association between postnatal maternal depressive symptoms and child attention problems. Perinatal maternal depressive symptoms were consistently associated with child brain development assessed 10 years later. These results suggest that the postnatal period is a window of vulnerability for adversities such as maternal depressive symptoms (Figure 8).

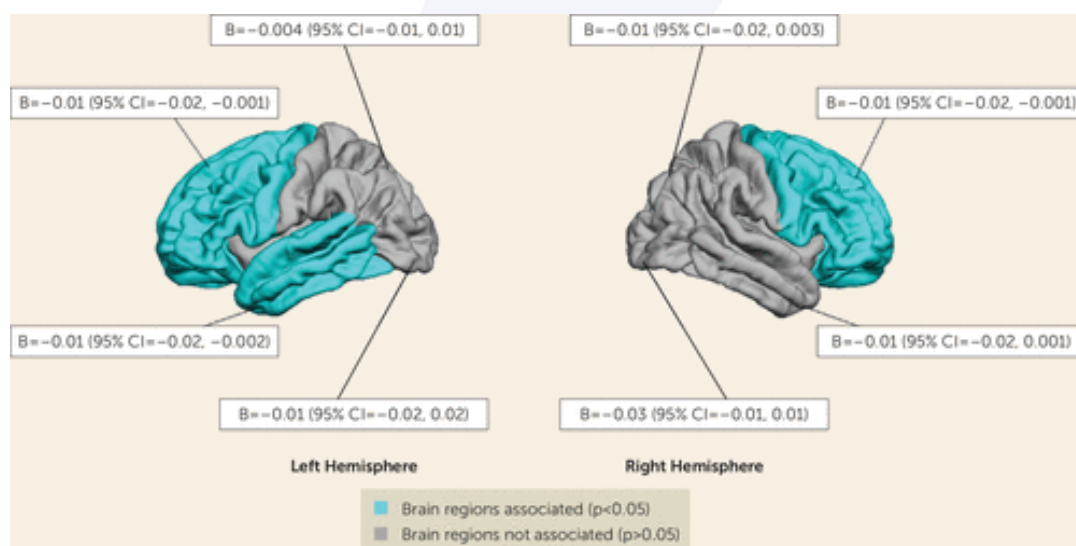


**Figure 8. Maternal depressive symptoms at child age 2 months and child cortical thickness at age 10 in a population-based study of maternal depressive symptoms and offspring brain development**

<sup>a</sup> Models were adjusted for child age at the time of MRI scanning (the mean age at scanning was 10.1 years [SD=0.6]), child sex, maternal ethnicity, maternal age at intake, maternal education level, marital status, household income, child birth weight, maternal smoking, and maternal alcohol use. B represents the difference in thickness, in millimeters.

#### Project 4: Maternal polyunsaturated fatty acids during pregnancy and offspring brain development in childhood (13)

**Involved partners:** ERASMUS

Emerging evidence suggests an association of maternal PUFA concentrations during pregnancy with child cognitive and neuropsychiatric outcomes such as intelligence and autistic traits. However, little is known about prenatal maternal polyunsaturated fatty acids (PUFAs) in relation to child brain development, which may underlie these associations. We



aimed to investigate the association of maternal PUFA status during pregnancy with child brain morphology, including volumetric and white matter microstructure measures. This study was embedded in a prospective population-based study. In total, 1553 mother-child dyads of Dutch origin were included. Maternal plasma glycerophospholipid PUFAs were assessed in mid-pregnancy. Child brain morphologic outcomes, including total gray and white matter volumes, as well as white matter microstructure quantified by global fractional anisotropy and mean diffusivity, were measured using MRI (including diffusion tensor imaging) at age 9–11 y. Maternal  $\omega$ -3 (n-3) long-chain PUFA (LC-PUFA) concentrations during pregnancy had an inverted U-shaped relation with child total gray volume (linear term:  $\beta$ : 16.7; 95% CI: 2.0, 31.5; quadratic term:  $\beta$ : -1.1; 95% CI: -2.1, -0.07) and total white matter volume (linear term:  $\beta$ : 15.7; 95% CI: 3.6, 27.8; quadratic term:  $\beta$ : -1.0; 95% CI: -1.8, -0.16). Maternal gestational  $\omega$ -6 LC-PUFA concentrations did not predict brain volumetric differences in children, albeit the linolenic acid concentration was inversely associated with child total white matter volume. Maternal PUFA status during pregnancy was not related to child white matter microstructure. Sufficient maternal  $\omega$ -3 PUFAs during pregnancy may be related to more optimal child brain development in the long term. In particular, exposure to lower  $\omega$ -3 PUFA concentrations in fetal life was associated with less brain volume in childhood. Maternal  $\omega$ -6 LC-PUFAs were not related to child brain morphology.

#### Project 5: Maternal prepregnancy body mass index and offspring white matter microstructure: results from three birth cohorts (14)

**Involved partners:** ERASMUS, UOULU

Prepregnancy maternal obesity is a global health problem and has been associated with offspring metabolic and mental ill-health. However, there is a knowledge gap in understanding potential neurobiological factors related to these associations. This study explored the relation between maternal prepregnancy body mass index (BMI) and offspring brain white matter microstructure at the age of 6, 10, and 26 years in three independent cohorts.

The study used data from three European birth cohorts ( $n = 116$  children aged 6 years,  $n = 2466$  children aged 10 years, and  $n = 437$  young adults aged 26 years). Information on maternal prepregnancy BMI was obtained before or during pregnancy and offspring brain white matter microstructure was measured at age 6, 10, or 26 years. We used magnetic resonance imaging-derived fractional anisotropy (FA) and mean diffusivity (MD) as measures of white matter microstructure in the brainstem, callosal, limbic, association, and projection tracts.

Linear regressions were fitted to examine the association of maternal BMI and offspring white matter microstructure, adjusting for several socioeconomic and lifestyle-related confounders, including education, smoking, and alcohol use (see **Figure 9**).

Maternal BMI was associated with higher FA and lower MD in multiple brain tracts, for example, association and projection fibers, in offspring aged 10 and 26 years, but not at 6 years. In each cohort maternal BMI was related to different white matter tract and thus no common associations across the cohorts were found.

Maternal BMI was associated with higher FA and lower MD in multiple brain tracts in offspring aged 10 and 26 years, but not at 6 years of age. Future studies should examine whether our observations can be replicated and explore the potential causal nature of the findings.

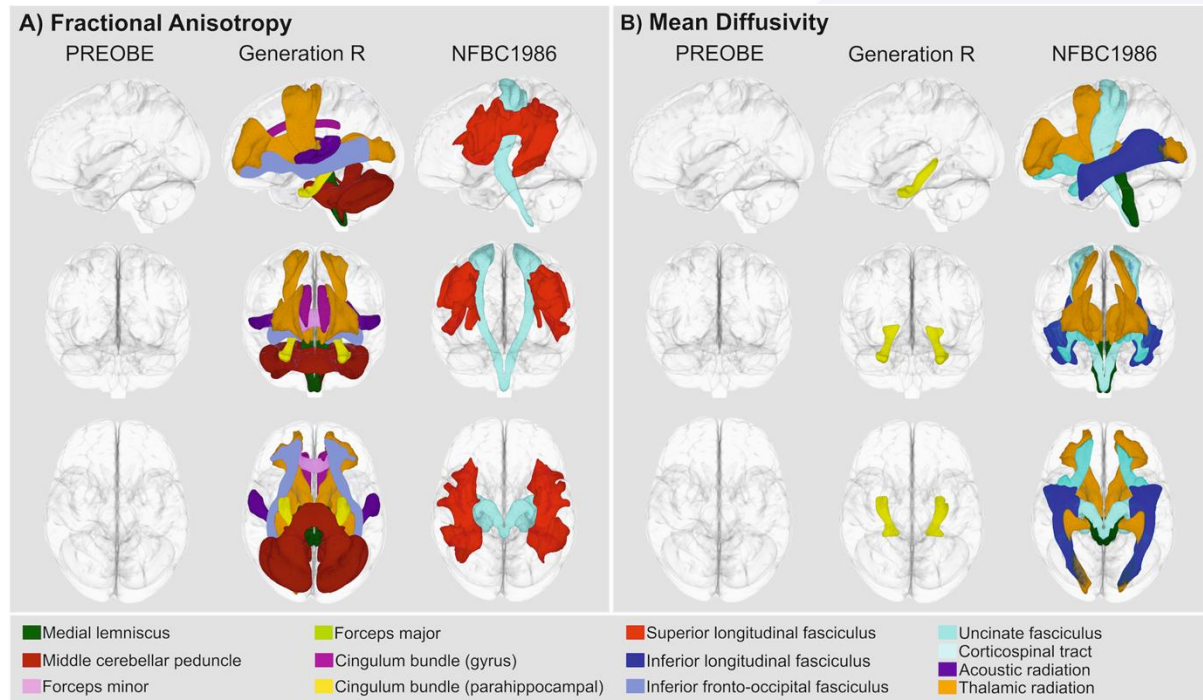


**Figure 9. White matter tracts associated with maternal BMI.** Only tracts surviving correction for multiple testing are presented. All models were adjusted for lifestyle and socioeconomic confounders including maternal age, smoking and drinking habits during pregnancy, maternal ethnicity, educational level, and birth weight, age and sex of the child. Panel a) represents fractional anisotropy and panel b) represents mean diffusivity. The images were created by averaging all individual maps by-tract in the NFBC 1986 sample and overlaying on a standardized brain template.

### Project 6: Prenatal exposure to organophosphate pesticides and brain morphology and white matter microstructure in preadolescents (15)

**Involved partners:** ERASMUS, ISGLOBAL

Prenatal exposure to organophosphate (OP) pesticides is associated with impaired neurodevelopment in humans and animal models. However, much uncertainty exists about the brain structural alterations underlying these associations. The objective of this study was to determine whether maternal OP pesticide metabolite concentrations in urine repeatedly measured during gestation are associated with brain morphology and white matter microstructure in 518 preadolescents aged 9–12 years.

Data came from 518 mother–child pairs participating in the Generation R Study, a population-based birth cohort from Rotterdam, the Netherlands. Maternal urine concentrations were determined for 6 dialkylphosphates (DAPs) including 3 dimethyl (DM) and 3 diethyl (DE) alkyl phosphate metabolites, collected at early, mid, and late pregnancy. At child's age 9–12 years, magnetic resonance imaging was performed to obtain T1-weighted images for brain volumes and surface-based cortical thickness and cortical surface



area, and diffusion tensor imaging was used to measure white matter microstructure through fractional anisotropy (FA) and mean diffusivity (MD). Linear regression models were fit for the averaged prenatal exposure across pregnancy.

DM and DE metabolite concentrations were not associated with brain volumes, cortical thickness, and cortical surface area. However, a 10-fold increase in averaged DM metabolite concentrations across pregnancy was associated with lower FA ( $B = -1.00$ ,  $95\%CI = -1.80, -0.20$ ) and higher MD ( $B = 0.13$ ,  $95\%CI = 0.04, 0.21$ ). Similar associations were observed for DE concentrations (**Figure 10**). This study provides the first evidence that OP pesticides may alter normal white matter microstructure in children, which could have consequences for normal neurodevelopment. No associations were observed with structural brain morphology, including brain volumes, cortical thickness, and cortical surface area.

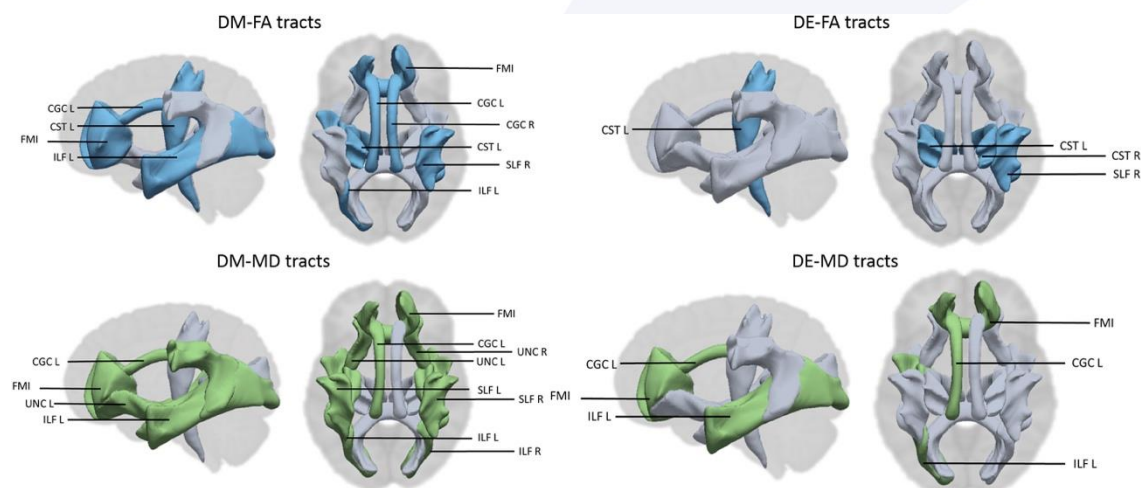


**Figure 10.** The white matter tracts of global fractional anisotropy (FA) and global mean diffusivity (MD) that are associated (blue = negative, green = positive) with <18 weeks, 18-25 weeks, and averaged: maternal dimethyl (DM) and diethyl (DE) alkyl phosphate metabolite concentrations in nmol/g creatinine. CGC= Cingulum bundle, CST = corticospinal tract, ILF = inferior longitudinal fasciculus, SLF = superior longitudinal fasciculus, UNC = uncinatus fasciculus, FMI = forceps minor, L = left hemisphere, R = right hemisphere.

### Project 7: Maternal early-pregnancy ferritin and offspring neurodevelopment: A prospective cohort study from gestation to school age (16)

**Involved partners:** ERASMUS

Iron plays a role in many key processes in the developing brain. During pregnancy, iron supplementation is widely recommended to prevent and treat iron deficiency; however, the prevalence of iron deficiency and the risk of iron overload vary greatly between populations. Evidence on the role of high levels of maternal ferritin, a storage iron marker during pregnancy in relation to offspring neurodevelopment is lacking.

Our main objective was to examine if maternal ferritin levels during pregnancy are associated with child cognitive and motor abilities.

We included Dutch mother-child dyads from the prospective population-based Generation R Study, born in 2002–2006. We compared children whose mothers had high (standard deviation score  $>+1$ ) or low (standard deviation score  $<-1$ ) early-pregnancy ferritin to children whose mothers had intermediate ferritin (reference group) using linear regression.

Children underwent non-verbal intelligence and language tests at 4–9 years (cognitive abilities), finger-tapping and balancing tests at 8–12 years (motor abilities), and structural magnetic resonance imaging at 8–12 years (brain morphology). Covariates were child age, sex, maternal intelligence quotient estimate, age, body-mass-index, education, parity, smoking and alcohol use.

Of the 2479 mother-child dyads with data on maternal ferritin and at least one child neurodevelopmental outcome, 387 mothers had low (mean = 20.6  $\mu\text{g/L}$ ), 1700 intermediate (mean = 64.6  $\mu\text{g/L}$ ) and 392 high (mean = 170.3  $\mu\text{g/L}$ ) early-pregnancy ferritin. High maternal ferritin was associated with 2.54 points (95% confidence interval -4.16, -0.92) lower child intelligence quotient and 16.02  $\text{cm}^3$  (95% confidence interval -30.57, -1.48) smaller brain volume. Results remained similar after excluding mothers with high C-reactive protein. Low maternal ferritin was not associated with child cognitive abilities. Maternal ferritin was unrelated to child motor outcomes.

High maternal ferritin during pregnancy was associated with poorer child cognitive abilities and smaller brain volume. Maternal iron status during pregnancy may be associated with offspring neurodevelopment.

#### Project 8: A prospective population-based study of gestational vitamin D status and brain morphology in preadolescents (17)

**Involved partners:** ERASMUS

Low vitamin D level during pregnancy has been associated with adverse neurodevelopmental outcomes such as autism spectrum disorders (ASD) in children. However, the underlying neurobiological mechanism remains largely unknown. This study investigated the association between gestational 25-hydroxyvitamin D [25(OH)D] concentration and brain morphology in 2597 children at the age of 10 years in the population-based Generation R Study. We studied both 25(OH)D in maternal venous blood in mid-gestation and in umbilical cord blood at delivery, in relation to brain volumetric measures and surface-based cortical metrics including cortical thickness, surface area, and gyrification using linear regression. We found exposure to higher maternal 25(OH)D concentrations in mid-gestation was associated with a larger cerebellar volume in children ( $b = 0.02$ , 95%CI 0.001 to 0.04), however this association did not remain after correction for multiple comparisons. In addition, children exposed to persistently deficient (i.e.,  $<25$  nmol/L) 25(OH)D concentration from mid-gestation to delivery showed less cerebral gray matter and white matter volumes, as well as smaller surface area and less gyrification at 10 years than those with persistently sufficient (i.e.,  $\geq 50$  nmol/L) 25(OH)D concentration (see **Figure 11**). These results suggest temporal relationships between gestational vitamin D concentration and brain morphological development in children.

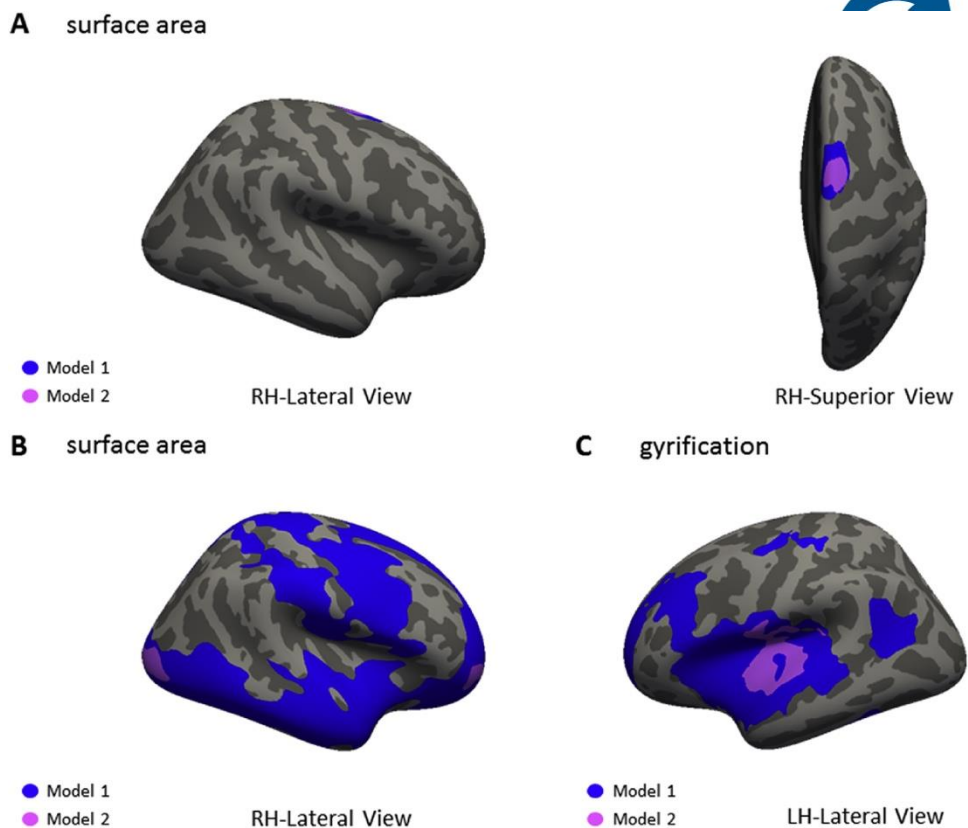


Figure 11. 25(OH)D status from mid-gestation to delivery in relation to surface-based cortical metrics in children at 10 years.

#### 4. Conclusion

The aim of Task 6.3 in the LifeCycle project is to report on the relationship of early life stressors with fetal and childhood brain developmental outcomes and the extent to which these mediate associations of early life exposures with mental health and psychopathology life course trajectories. Stressors in this context include those introduced through socio-economic, migration, urban environment, and lifestyle factors. In conclusion, these papers collectively show that early factors in pregnancy and childhood may affect brain development, and that these differences in brain morphology may mediate child cognitive and behavioral outcomes.

#### 5. Contribution of partners

In the above-mentioned projects, three partners were able to contribute, which were the Erasmus MC, ISGlobal and UOULU.

- **ERASMUS:** led task 6.3, contributed to all the projects from 3.1, 3.2, 3.3 and 3.4
- **ISLGOBAL:** contributed to all projects from 3.1 and 3.2 and to projects 3.3.1 and 3.4.6.
- **UOULU:** contributed to project 3.4.5

We also performed multi-cohort analyses and published papers with other institutes (University Utrecht, Leiden University, University of Granada). Unfortunately, the number of partners that contributed to the projects is limited due to the fact that only a small number of cohorts have neuroimaging data available and possibilities for harmonization.



## 6. Deviations from original plan

This deliverable has been fulfilled fully in line with the original plan as stated in the GA.

## 7. Dissemination activities

The results of these projects have been presented at national and international conferences.

- Dr. Sara Sammalahhti presented her work on ferritin and brain developmental outcomes at the Obstetrics and Gynecology Department at the Helsinki and Uusimaa Hospital district in a monthly research meeting on Jan 31st.
- Dr. Runyu Zou presented his work related to this work package at the American Association of Child and Adolescent Psychiatry's 66th Annual Meeting, Chicago, USA, 2019, and the Sophia Research Day 2020.
- Dr. Andrea Cortes presented her work on attachment and brain morphology at the biennial Meeting of the Society in Research on Child Development (SRCO 2019).
- Dr. Carolina Silva shared her publications in her professional network using LinkedIn, and she presented her work at the Sophia Children's Hospital Research Day in April 2021 and the yearly Dutch Epidemiology Conference (WEON) in June 2021.
- Findings on exposure to air pollution and brain development was discussed with the municipality of Rotterdam (website in Dutch: <https://www.pzc.nl/rotterdam/oproep-pak-fijnstof-aan-om-hersenschade-bij-baby-s-te-voorkomen~ade83a6d/?referrer=https%3A%2F%2Fwww.google.com%2F>). Furthermore, there was a lot of media coverage on these air pollution findings.
  - For example, Monica Guxens was interviewed after publication of the paper on air pollution and brain structure in young children (<https://www.usnews.com/news/national-news/articles/2018-03-14/air-pollution-within-levels-considered-safe-changes-brain-development-leads-to-cognitive-impairment>). Dr. Guxens presented her work on air pollution and brain morphology outcomes at several international conferences. She had oral presentations at the 10th World Congress Developmental Origins of Health and Disease. Rotterdam, The Netherlands in 2017, XXXVI Scientific Meeting of the Spanish Society of Epidemiology. Lisbon, Portugal in 2018, ISES-ISEE 2018 Joint Annual Meeting. Ottawa, Canada in 2018, and the 3rd Early Career Researchers Conference on Environmental Epidemiology, Freising, Germany in 2018, and at the 30<sup>th</sup> Conference of the International Society for Environmental Epidemiology. Utrecht, The Netherlands. The work in radiofrequency electromagnetic fields exposure and brain developmental outcomes was presented in 2019 at the XXXVII Scientific Meeting of the Spanish Society of Epidemiology. Oviedo, Spain, as well as a poster presentation at the Bioelectromagnetics Conference. Montpellier, France.
- Hanan El Marroun presented at society of Epidemiology research (SPER) and received a prize for the paper on gestational age and brain morphology (SPER Heinz Berendes Travel Award 2020 for the annual meeting Society Perinatal Epidemiology research). Further, Hanan El Marroun teaches on developmental psychology yearly

- (Bachelor students), where she also presents the findings from several of these LifeCycle studies in her lecture on prenatal influences and brain development. Finally, Hanan El Marroun also uses social media to disseminate knowledge to a broad audience ([https://www.instagram.com/hersen\\_onderzoeker/](https://www.instagram.com/hersen_onderzoeker/)).

## 8. References

1. Guxens M, Lubczyńska MJ, Muetzel RL, Dalmau-Bueno A, Jaddoe VWV, Hoek G, et al. Air Pollution Exposure During Fetal Life, Brain Morphology, and Cognitive Function in School-Age Children. *Biological Psychiatry*. 2018;84(4):295-303.
2. Lubczyńska MJ, Muetzel RL, El Marroun H, Hoek G, Kooter IM, Thomson EM, et al. Air pollution exposure during pregnancy and childhood and brain morphology in preadolescents. *Environmental Research*. 2021;198:110446.
3. Lubczyńska MJ, Muetzel RL, El Marroun H, Basagaña X, Strak M, Denault W, et al. Exposure to Air Pollution during Pregnancy and Childhood, and White Matter Microstructure in Preadolescents. *Environmental Health Perspectives*. 2020;128(2):27005.
4. Birks LE, van Wel L, Liorni I, Pierotti L, Guxens M, Huss A, et al. Radiofrequency electromagnetic fields from mobile communication: Description of modeled dose in brain regions and the body in European children and adolescents. *Environmental Research*. 2021;193:110505.
5. Cabré-Riera I, El Marroun H, Muetzel R, van Wel L, Liorni I, Thielens A, et al. Estimated whole-brain and lobe-specific radiofrequency electromagnetic fields doses and brain volumes in preadolescents. *Environment International*. 2020;142:105808.
6. Alemany S, Jansen PR, Muetzel RL, Marques N, El Marroun H, Jaddoe VWV, et al. Common Polygenic Variations for Psychiatric Disorders and Cognition in Relation to Brain Morphology in the General Pediatric Population. *Journal of the American Academy of Child & Adolescent Psychiatry*. 2019;58(6):600-7.
7. Cortes Hidalgo AP, Muetzel R, Luijk PCM, Bakermans-Kranenburg MJ, El Marroun H, Vernooij MW, et al. Observed infant-parent attachment and brain morphology in middle childhood—A population-based study. *Developmental Cognitive Neuroscience*. 2019;40:100724.
8. Silva CCV, Jaddoe VWV, Muetzel RL, Santos S, El Marroun H. Body fat, cardiovascular risk factors and brain structure in school-age children. *Int J Obes*. 2021;45:2425–2431.
9. El Marroun H, Klapwijk ET, Koevoets M, Brouwer RM, Peters S, van't Ent D, et al. Alcohol use and brain morphology in adolescence: A longitudinal study in three different cohorts. *European Journal of Neuroscience*. 2021;54(6):6012-26.
10. El Marroun H, Zou R, Leeuwenburg MF, Steegers EAP, Reiss IKM, Muetzel RL, et al. Association of Gestational Age at Birth With Brain Morphometry. *JAMA Pediatr*. 2020;174(12):1149–58.
11. Silva CCV, El Marroun H, Sammallahti S, Vernooij MW, Muetzel RL, Santos S, Jaddoe VWV. Patterns of Fetal and Infant Growth and Brain Morphology at Age 10 Years. *JAMA Netw Open*. 2021;4(12):e2138214.



12. Zou R, Tiemeier H, van der Ende J, Verhulst FC, Muetzel RL, White T, et al. Exposure to Maternal Depressive Symptoms in Fetal Life or Childhood and Offspring Brain Development: A Population-Based Imaging Study. *Am J Psychiatry*. 2019;176(9):702-10.
13. Zou R, El Marroun H, Voortman T, Hillegers M, White T, Tiemeier H. Maternal polyunsaturated fatty acids during pregnancy and offspring brain development in childhood. *American Journal of Clinical Nutrition*. 2021;114(1):124-33.
14. Verdejo-Román J, Björnholm L, Muetzel RL, Torres-Espínola FJ, Lieslehto J, Jaddoe VW, et al. Maternal prepregnancy body mass index and offspring white matter microstructure: results from three birth cohorts. *Int J Obes*. 2019;43:1995–2006.
15. Van den Dries MA, Lamballais S, El Marroun H, Pronk A, Spaan S, Ferguson KK, et al. Prenatal exposure to organophosphate pesticides and brain morphology and white matter microstructure in preadolescents. *Environmental Research* 2020;191:110047.
16. Sammallahhti S, Tiemeier H, Reiss IKM, Muckenthaler MU, El Marroun H, Vermeulen M. Maternal early-pregnancy ferritin and offspring neurodevelopment: A prospective cohort study from gestation to school age. *Paediatric and Perinatal Epidemiology*. 2022;36(3):425-34.
17. Zou R, El Marroun H, McGrath JJ, Muetzel RL, Hillegers M, White T, Tiemeier H. A prospective population-based study of gestational vitamin D status and brain morphology in preadolescents. *NeuroImage*. 2020;209:116514.

## Appendix 1

### Harmonization recommendations for Neuroimaging data

#### 1. Aim of task WP 6.3

The aim of Work Package 6, Task 3 of LifeCycle is to 'Identify early brain development that mediates the relationships between early-life stressors and later mental health and disease'. For this purpose, it is important to harmonize the neuroimaging data that has been collected and potential future neuroimaging data collection within the EU Child Cohort Network.

The aim of this specific neuroimaging protocol is to guide the cohorts in the harmonization process to generate variables that will be comparable across cohorts and measurements. The harmonization strategy is based on an adaptation of the DataSHaPER guidelines [1], aimed to facilitate a rigorous, transparent and effective harmonization, made in the framework of the MeDALL project [2], like in the complete work package (WP 6), as well as neuroimaging networks that are existing (e.g ENIGMA, <http://enigma.ini.usc.edu>).

#### 2. Neuroimaging domains

The following table provides a short description of the neuroimaging outcome domains. We have not assigned any priority yet, because there are only a few cohorts that have neuroimaging data. In addition, the neuroimaging data was assessed at very different ages ranges. Because it is very hard to share surface-based data and MRI images (need for large storage), the first step is to harmonize summary variables in the LifeCycle project.

Neuroimaging domains	Dimensions	Definitions (different levels of complexity depending on age)
Structural neuroimaging	Volumetric data in mm <sup>3</sup>	Preferably processed through Freesurfer v 6.0
	Cortical surface area in mm <sup>2</sup>	Preferably processed through Freesurfer v 6.0
	Cortical thickness in mm	Preferably processed through Freesurfer v 6.0
	Gyrification Index	Preferably processed through Freesurfer v 6.0
	Surface-based data	Preferably processed through Freesurfer v 6.0
Diffusion weighted neuroimaging	Fractional anisotropy	Mean FA values per tract; preferably processed using standard tools in combination with the AutoPtx software [1-5] <a href="https://fsl.fmrib.ox.ac.uk/fsl/fslwiki/AutoPtx">https://fsl.fmrib.ox.ac.uk/fsl/fslwiki/AutoPtx</a>
	Diffusivity measures	Mean MD, RD and AD values per tract; preferably processed using standard tools in combination with the AutoPtx software MD: mean diffusivity AD: axial diffusivity RD: radial diffusivity
Resting-state functional neuroimaging	Summary measures quantifying fluctuations in the connectivity time courses	<i>Ongoing process in Generation R</i> Whole brain dynamic functional network connectivity (DFNC)
	Summary stats based on graph theory	Global efficiency, shortest path length, number of nodes and edges
Task-related functional neuroimaging	Dependent on tasks and specific cohorts	

### 3. Time periods variables

Neuroimaging data has only been collected in a few cohorts, namely ALSPAC, the Generation R Study, Norwegian Mother and Child Cohort Study (MOBA), Northern Finnish Birth Cohort (NFBC1966 and. NFBC1986). In Generation R Next, neuroimaging data will be collected in new-borns (planned assessment). We may need to adjust the inventory for this cohort in a later phase of the study. However, age range goes beyond 18 years, while in Lifecycle the focus is on children up to 18 years.

**Table 1: Cohorts with neuroimaging information**

Cohort	0-5 yrs.	5-10 yrs.	10-13 yrs.	13-15 yrs.	15-20 yrs.	20-25 yrs.	25-30 yrs.	30+ yrs.
ALSPAC						X		
The Generation R Study		X	X	X	(X)			
NFBC1966								X
MOBA	X	X	X					
NFBC1986						X	X	
Generation R Next	(X)							

X: data available

(X): planned data collection

Age range after 18 years

Based on group consensus in WP6 (June/July 2020), the harmonization of the neuroimaging data will be similar to the harmonization of the behavioural outcomes, and will be on a yearly basis up to 30 years. Cohorts will only make the variables in the ages where data if is available. If no MRI data is available, e.g. at 4 years in the Generation R or ALSPAC cohort, then this variable will not be constructed.



#### 4. Technical details neuroimaging

For now, technical information is only partly available. See tables below.

**Table 2: Technical parameters of the acquired structural magnetic resonance imaging (T1)**

	MOBA	MOBA	Generation R	Generation R	Generation R	ALSPAC	NFBC1986	NFBC1966
Age range	4-10 years	4-10 years	6-9 years	9-12 years	13-14 years	20-25	20-30 years	33-44 years
Number of	¿?	¿?	1070	3992	On-going	800 **	329/471***	188/285***
Scanner	¿?	¿?	3T GE	3T GE	3T GE	3T GE HDx	1.5 T	1.5 TGE
Head coil	¿?	¿?	8	8	8	8	8	8
Sequence type	¿?	¿?	IR-FSPGR	IR-FSPGR	IR-FSPGR			3D-SPGR
TR (ms)	¿?	¿?	10.3	877	877	7.8		35
TE (ms)	¿?	¿?	4.2	3.4	3.4	3.0		5.0
TI (ms)	¿?	¿?	350	600	600			
NEX	¿?	¿?	1					
Flip angle (°)	¿?	¿?	16	10	10			35
FOV	¿?	¿?		220 x 220	220 x 220			
Matrix	¿?	¿?	256 x 256	220 X220	220 X220			
Voxel size (mm <sup>3</sup> )	¿?	¿?	0.9 x 0.9 x	1.0 x 1.0 x	1.0 x 1.0 x 1.0	1.0 x 1.0 x	1.0 x 1.0 x	1.0 x 1.0 x
Accelerating factor	¿?	¿?	2	2	2			
Acquisition time	¿?	¿?	5 min 40 s	5 min 40 s	5 min 40			
Post-processing	¿?	¿?	Freesurfer	Freesurfer v	Freesurfer v			Freesurfer
IR-FSPGR: Intense Inversion Recovery Fast Spoiled Gradient Recalled, T1 weighted image; TR, Repetition Time; TE, Echo Time; TI, Inversion Time 3D fast spoiled gradient echo sequence - ALSPAC; 3D SPGR : three dimensional spoiled gradient echo;								

**Table 3: Technical parameters of the acquired diffusion weighted images (DTI)**

	MOBA	MOBA	Generation R	Generation R	Generation R	ALSPAC	NFBC1986	NFBC1966
Age range	4-10 years	4-10 years	6-9 years	9-12 years	13-14 years	20-25 years	20-30	33-44 years
Number of	¿?	¿?	1070	3777	On-going		329/471	188/285
Scanner	¿?	¿?	3T GE	3T GE	3T GE	3T GE HDx	1.5 T	
Sequence type	¿?	¿?	EPI					
Head coil	¿?	¿?	8	8	8	8	8	
TR (ms)	¿?	¿?	11000	12500	12500		9000	
TE (ms)	¿?	¿?	8	72	72	87	102	
FOV (mm)	¿?	¿?	256 x 256	240 x 240	240 x 240	230 x 230	192 x 192	
Matrix size	¿?	¿?	128 x 128	120 x120	120 x120	96 x96	104 x 104	
Number of slices	¿?	¿?	77	65	65		61	
Voxel size	¿?	¿?	2 x 2 x 2	2 x 2 x 2	2 x 2 x 2	2.4 x 2.4 2.4	2.3 x 2.3 x	
Directions	¿?	¿?	35	35	35	60	64/32?	64/32?
b-value	¿?	¿?	0 s/mm <sup>2</sup>	900	900	1200 s/mm <sup>2</sup>	1000	1000
Acquisition time	¿?	¿?	7 min 40 s	7 min 40 s	7 min 40 s		8 min 25 s	
Pre-processing	¿?	¿?	FSL, FMRIB,	FSL, FMRIB,	FSL, FMRIB,	Explore DTI		
Post-processing	¿?	¿?	Tractography	Tractography	Tractography	Tractography,		
EPI: echo planar imaging								

## 5. Instructions to harmonize variables

- Identify the cohort-specific instruments that measure the main neuroimaging domains. We advise to all use the same software and the same pipeline to produce the variables when possible. Generation R has been using FreeSurfer version 6.0 for structural processing (**see Annex I**) and for diffusion weighted image processing the Generation R study used Autoptx (**see Annex II**). For functional MRI (task-related and resting-state), quality assessment is also important, but currently there are no recommendations for specific ways to process the data. In Generation R standard tools have been used from the FSL-package.
- In order to be as consistent as possible, it is important to more or less perform the quality assessment in similar ways. In the Generation R, there is some information on how the quality assessment was done for the T1 and DTI images and this can be shared upon request. There are also several automated QA tools available online, that we might consider to start using in the cohorts.
- For each harmonized assessment, it is important to provide the exact age in years of when the assessment took place.; this will facilitate developing trajectories.
- For volumetric measures make sure we keep the original data of Freesurfer; volumes in mm<sup>3</sup>, surface are in mm<sup>2</sup> and thickness in mm. Do not convert the volumes in other scales (e.g. cm<sup>3</sup> or cm<sup>2</sup>). For diffusion weighted measures, also keep the same scales, (e.g. FA ranges from 0 to 1). In this case standardization of the measures is not needed, and outcomes remain interpretable.
- Provide a description of the harmonized variables, including: cohort name, domain, dimension, harmonized variable, description, source variables, data type, interpretation original score, evaluator, number of subjects, syntax, and date of update (See Annex II. Example: Description of harmonized variables). You will find attached the template file to provide this information.
- Future actions related to harmonization process: if there are cohorts that are going to collect neuroimaging it is good to use similar sequences when possible and the same software packages for processing.
- For the analyses, batch effects can be considered with the COMBAT tools; this tool has been used in structural MRI data, as well as diffusion MRI data [6-7], and is freely available on GitHub: <https://github.com/Jfortin1/ComBatHarmonization>
- The focus will be on the core neuroimaging outcome, which are key volumetric measures: estimated intracranial volume, total gray matter, total white matter, cerebellum, amygdala and hippocampal volume.
- For instructions on quality control after the harmonization, use the instructions that were used for the variables harmonized previously in WP6 starting on page 36 in the WP6 harmonization protocol. Step 1 verify list of variables and formats, step 2 check univariate distributions, step 3 check internal validation, step 4 check quality for repeated measures, step 5 complete the online catalogue.

## 6. References

- [1] De Groot M, Vernooij MW, Klein S, Ikram MA, Vos FM, Smith SM, Niessen WJ, Andersson JLR, 2013. Improving alignment in Tract-based spatial statistics: Evaluation and optimization of image registration. *NeuroImage*, 76, 400-411.
- [2] Mori S, Kaufmann WE, Davatzikos C, Stieltjes B, Amodei L, Fredericksen K, Pearlson GD, Melhem ER, Solaiyappan M, Raymond GV, Moser HW, Van Zijl PCM, 2002. Imaging cortical association tracts in the human brain using diffusion-tensor-based axonal tracking. *Magnetic Resonance in Medicine* 47, 215–223.
- [3] Stieltjes B, Kaufmann WE, Van Zijl PC, Fredericksen K, Pearlson GD, Solaiyappan M, Mori S, 2001. Diffusion tensor imaging and axonal tracking in the human brainstem. *NeuroImage* 14, 723–735.
- [4] Wakana S, Caprihan A, Panzenboeck MM, Fallon JH, Perry M, Gollub RL, Hua K, Zhang J, Jiang H, Dubey P, Blitz A, Van Zijl P, Mori S, 2007. Reproducibility of quantitative tractography methods applied to cerebral white matter. *NeuroImage* 36, 630–644.
- [5] Wakana S, Jiang H, Nagae-Poetscher LM, Van Zijl PCM, Mori, S, 2004. Fiber Tract-based Atlas of human white matter anatomy. *Radiology* 230, 77–87
- [6] Fortin JP, Parker D, Tunc B, Watanabe T, Elliott MA, Ruparel K, Roalf DR, Satterthwaite TD, Gur RC, Gur RE, Schultz RT, Verma R, Shinohara RT, 2017. Harmonization Of Multi-Site Diffusion Tensor Imaging Data. *NeuroImage*, 161, 149-170.
- [7] Fortin JP, Cullen N, Sheline YI, Taylor WD, Aselcioglu I, Cook PA, Adams P, Cooper C, Fava M, McGrath PJ, McInnis M, Phillips ML, Trivedi MH, Weissman MM, Shinohara RT, 2018. Harmonization of cortical thickness measurements across scanners and sites. *NeuroImage*, 167, 104-120.



## Annex I Freesurfer information

### General

FreeSurfer is a software package for the analysis and visualization of structural and functional neuroimaging data from cross-sectional or longitudinal studies. General information about the software can be found on the FreeSurfer Wikipage:

<https://surfer.nmr.mgh.harvard.edu/fswiki/FreeSurferWiki>

### Download and installation

Information about downloading and installing FreeSurfer:

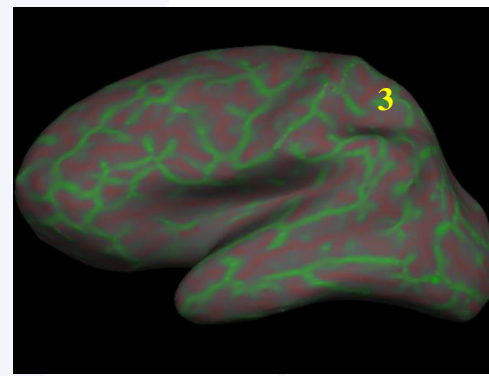
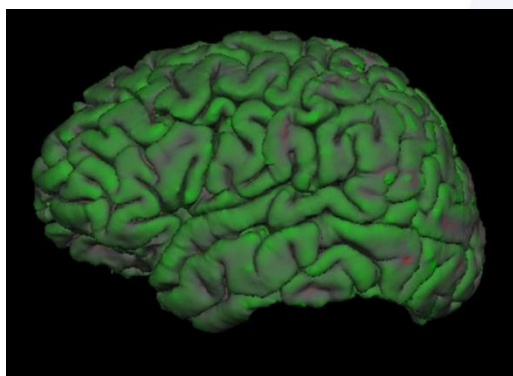
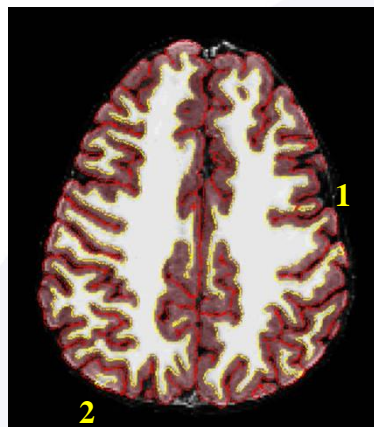
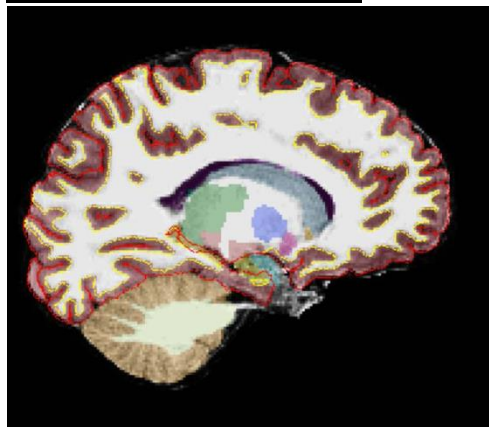
<https://surfer.nmr.mgh.harvard.edu/fswiki/DownloadAndInstall>

### Steps to run FreeSurfer on your data:

1. Refer to your subject in your data folder  
SUBJECT="R112594"  
EVENT="100015"
2. make the directory that FreeSurfer will look in for the MGZ file, and  
mkdir -p \${MRDATA}/structural/\${SUBJECT}/mri/orig
3. convert from DICOM to MGZ  
mri\_convert -it dicom -ot mgz  
\${MRDATA}/dicom/\${SUBJECT}/\${EVENT}/IRFSPGR\*/\*0001.dcm  
\${MRDATA}/structural/\${SUBJECT}/mri/orig/001.mgz
4. kick-off FreeSurfer on the subject  
recon-all -s \${SUBJECT} -autorecon-all

Depending on the hardware running FreeSurfer takes about 20-24 hours per subject. Depending on the quality data, it may be necessary to add flags to the command (<https://surfer.nmr.mgh.harvard.edu/fswiki/recon-all> ) or to manually correct topologies.

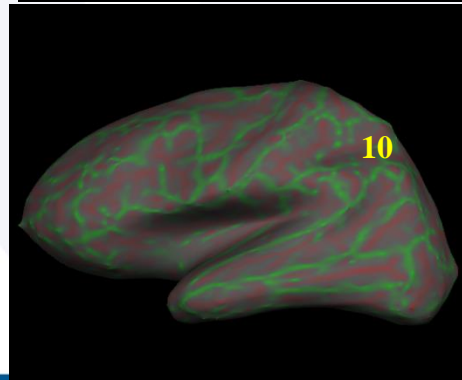
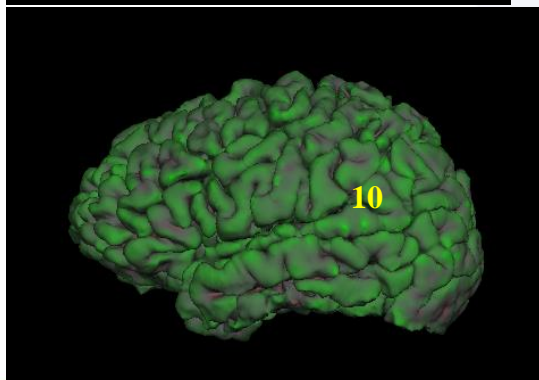
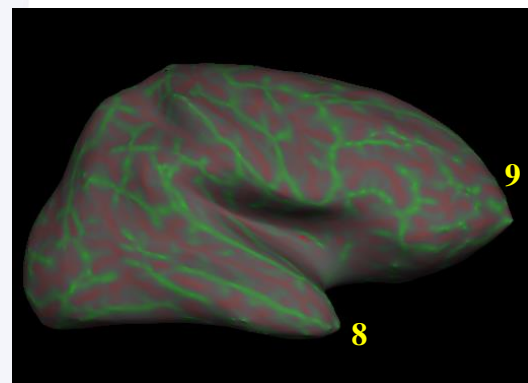
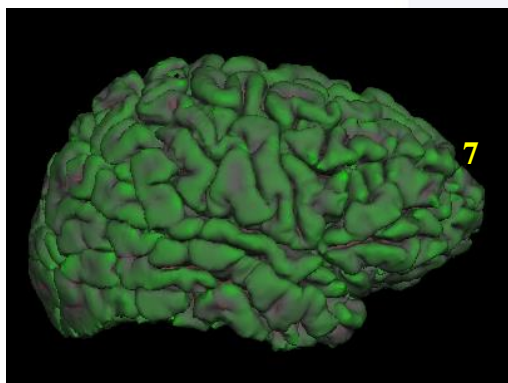
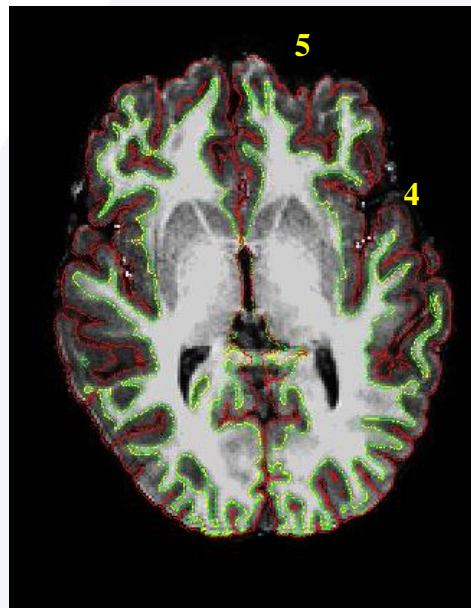
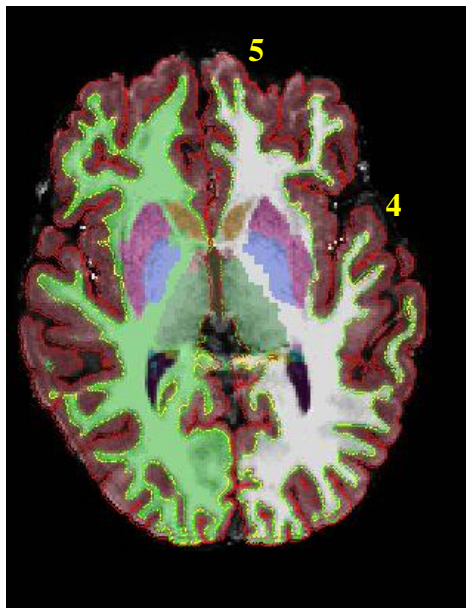
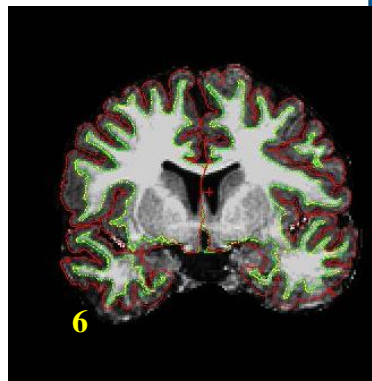
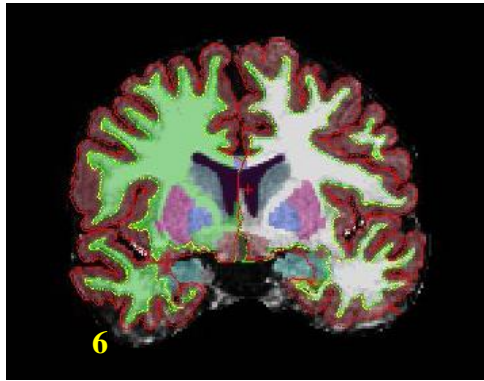
Freesurfer output checking  
Example of a good dataset:



**Why this is a good quality Freesurfer output:**

In this example, you see that the white matter and the grey matter lining follows the image correctly. Little mistakes in the 2D image are visible (1 and 2), but if this in a few slices, then this is not a problem. The 3D pial image looks smooth and there are little intense colored areas visible on both the 3D pial image as well as the 3D inflated image looks smooth.

Note that there is a difference in the shape of the inflated surface when comparing it to the adult inflated surface (bert). The inflated surface of pediatric data does have a bump in the occipital area (3), which looks off, but as long the surface is smooth this should not be a problem. Data with good quality will be used in the analyses.



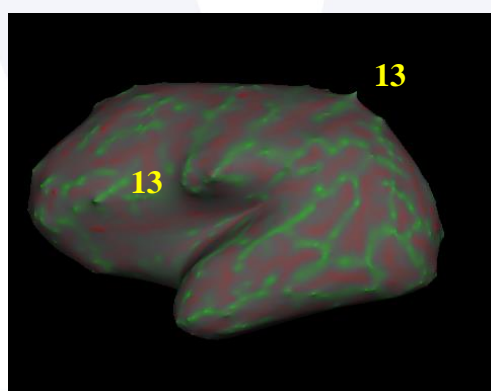
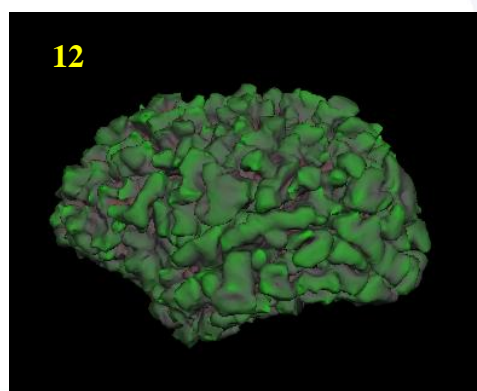
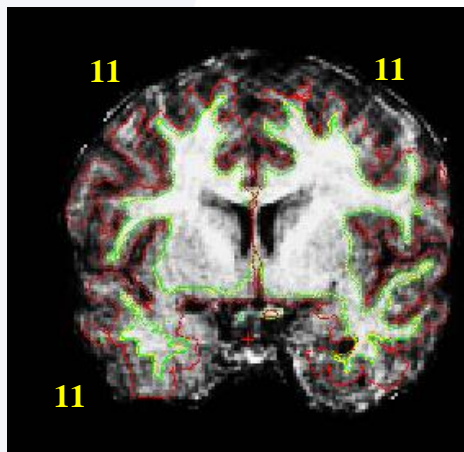
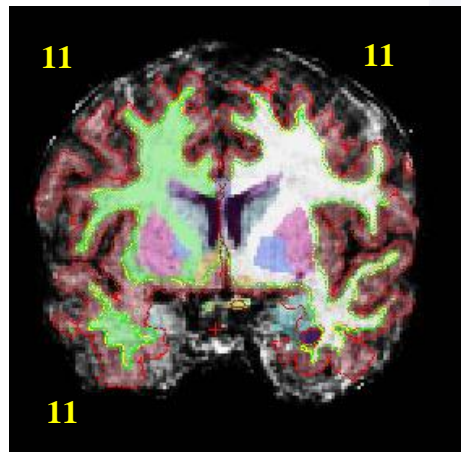


**Why this is a questionable quality Freesurfer output:**

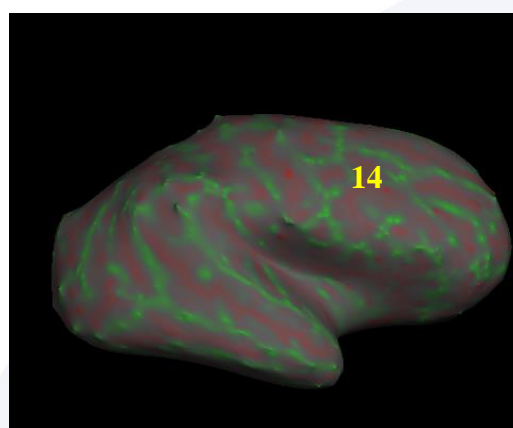
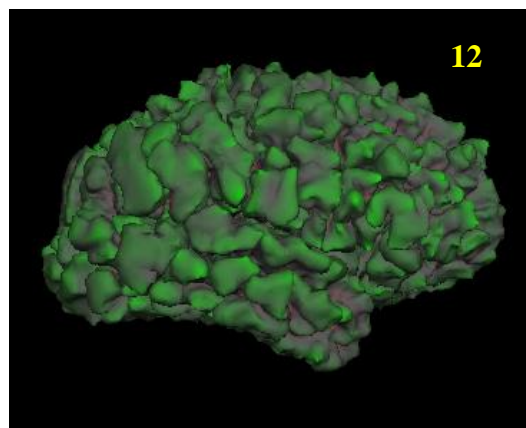
In this example, you see that overall the white matter and the grey matter lining follow the image. However, there are some areas where the lining could be better, sometimes the grey matter does not follow the surface correctly (4) and you can also see this in the white matter lining (5). When you see this in one or two slices that should not be a problem, but when you see this at multiple slices then this means you miss a significant proportion of the grey and white matter.

Specifically, the temporal lobe has this problem more often and is therefore separately rated (6).

In this case, the accumulation of the little mistakes can be seen in the 3D pial surface image, where little chunks of gyri (7) are missing. In particular, the frontal area does not look smooth like the good quality image, but the surface looks chunky, rocky or bumpy. Although the 3D inflated surface looks smooth, you do see some spikes (the frontal area and the temporal area looks spiky, 8,9) and intense colored spots are visible on the pial and the inflated surface (10) as well. Although the data is not perfect (questionable) it is of sufficient quality to be used in the analyses. It is expected that a large proportion of the pediatric data will be of this quality.







**Why this is a poor quality Freesurfer output:**

In this example, you see that that overall the white matter and the grey matter lining do not follow the image (11). Actually, the quality of the input image is very blurry and even a manual segmentation would have been impossible. The rings that you see are due to movement. It is very clear that the red line does not follow the grey matter at all.

Again, you can see the accumulation of all the mistakes the 3D pial surface image, where the surface looks completely chunky or rocky (12). You do not recognize a brain in this image. Further, the 3D inflated surface does not look smooth and there is a lot of spiking (13) and intense colored spots (14) on the inflated surface are clearly visible as well. We will not use data with poor quality output in the analyses.



## Annex II AutoPtx

Information on the AutoPtx package can be found:

<https://fsl.fmrib.ox.ac.uk/fsl/fslwiki/AutoPtx>

AutoPtx v0.1.1 is a set of simple scripts and mask images to run probabilistic tractography in subject-native space using pre-defined protocols. AutoPtx requires a working version of FSL and has been tested on Linux and Mac.

To run this package, FSL should be working. If the FSL package is not installed; one can find this here: <https://fsl.fmrib.ox.ac.uk/fsl/fslwiki>

The AutoPtx software package can calculate average FA, MD, RD and AD for the main white matter tracts. These include: brain stem tracts, projection fibers, association fibers, limbic system fibers and callosal fibers.

Diffusion image processing was conducted using DTIPrep tool (<https://www.nitrc.org/projects/dtiprep/>) by inspecting a combination of manual and automated checks, including examining slice wise variation in the diffusion signal, examining the sum-of-squares error of the tensor calculation, and inspecting intersubject registration accuracy.



**Annex III Harmonization table variables**

For cerebellum volume, first compute sum of cerebellar cortex and white matter volume for left and right hemisphere.

- **List of yearly intervals variables**

	Variable name	Label description	Values	Unit	Datatype	comments
<b>META-VARIABLES</b>						
Child identifier	Child_id	Unique identifier number for the index child				Either the original id or a new id generated by the cohort; Should already be created for the core variable list, please add here to make it possible to combine data
<b>BRAIN VOLUMES</b>						
Estimated intracranial volume	etiv_0 etiv_1 etiv_2 etiv_3 etiv_4 etiv_5 etiv_6 etiv_7 etiv_8 etiv_9 etiv_10 etiv_11 etiv_12 etiv_13	Estimated intracranial volume at age 0-1 years Estimated intracranial volume at age 1-2 years Estimated intracranial volume at age 2-3 years Estimated intracranial volume at age 3-4 years Estimated intracranial volume at age 4-5 years Estimated intracranial volume at age 5-6 years Etc..		mm <sup>3</sup>	Continuous, rounded without decimals	Based on freesurfer v 6.0 output data (aseg file)

	etiv_14 etiv_15 etiv_16 etiv_17 .... etiv_30					
Total gray matter	TotalGrayVol_0 TotalGrayVol_1 TotalGrayVol_2 TotalGrayVol_3 TotalGrayVol_4 TotalGrayVol_5 TotalGrayVol_6 TotalGrayVol_7 TotalGrayVol_8 TotalGrayVol_9 TotalGrayVol_10 TotalGrayVol_11 TotalGrayVol_12 TotalGrayVol_13 TotalGrayVol_14 TotalGrayVol_15 TotalGrayVol_16 TotalGrayVol_17 ... TotalGrayVol_30	Total gray matter volume at age 0-1 years Total gray matter volume at age 1-2 years Total gray matter volume at age 2-3 years Total gray matter volume at age 3-4 years Total gray matter volume at age 4-5 years Total gray matter volume at age 5-6 years  Etc..		mm <sup>3</sup>	Continuous, rounded without decimals	Based on freesurfer v 6.0 output data (aseg file)
Total white matter	CerebralWhiteMatterVol_0 CerebralWhiteMatterVol_1	Cerebral white matter volume at age 0-1 years Cerebral white matter volume at age 1-2 years		mm <sup>3</sup>	Continuous, rounded without decimals	Based on freesurfer v 6.0 output data (aseg file)



CerebralWhiteMatterVol_2	Cerebral white matter volume at age 2-3 years				
CerebralWhiteMatterVol_3	Cerebral white matter volume at age 3-4 years				
CerebralWhiteMatterVol_4	Cerebral white matter volume at age 4-5 years				
CerebralWhiteMatterVol_5	Cerebral white matter volume at age 5-6 years				
CerebralWhiteMatterVol_6	Etc..				
CerebralWhiteMatterVol_7					
CerebralWhiteMatterVol_8					
CerebralWhiteMatterVol_9					
CerebralWhiteMatterVol_10					
CerebralWhiteMatterVol_11					
CerebralWhiteMatterVol_12					
CerebralWhiteMatterVol_13					
CerebralWhiteMatterVol_14					
CerebralWhiteMatterVol_15					
CerebralWhiteMatterVol_16					

	CerebralWhiteMatterVol_17 ... CerebralWhiteMatterVol_30					
Amygdala	Right-amygdala_0 Right-amygdala_1 Right-amygdala_2 Right-amygdala_3 Right-amygdala_4 Right-amygdala_5 Right-amygdala_6 Right-amygdala_7 Right-amygdala_8 Right-amygdala_9 Right-amygdala_10 Right-amygdala_11 Right-amygdala_12 Right-amygdala_13 Right-amygdala_14 Right-amygdala_15 Right-amygdala_16 Right-amygdala_17 ... Right-amygdala_30	Right amygdala volume at age 0-1 years Right amygdala volume at age 1-2 years Right amygdala volume at age 2-3 years Right amygdala volume at age 3-4 years Right amygdala volume at age 4-5 years Right amygdala volume at age 5-6 years  Etc..		mm <sup>3</sup>	Continuous, rounded without decimals	Based on freesurfer v 6.0 output data (aseg file)
	Left-amygdala_0 Left-amygdala_1 Left-amygdala_2 Left-amygdala_3 Left-amygdala_4	Left amygdala volume at age 0-1 years Left amygdala volume at age 1-2 years Left amygdala volume at age 2-3 years Left amygdala volume at age 3-4 years Left amygdala volume at age 4-5 years		mm <sup>3</sup>	Continuous, rounded without decimals	Based on freesurfer v 6.0 output data (aseg file)

	Left-amygdala_5 Left-amygdala_6 Left-amygdala_7 Left-amygdala_8 Left-amygdala_9 Left-amygdala_10 Left-amygdala_11 Left-amygdala_12 Left-amygdala_13 Left-amygdala_14 Left-amygdala_15 Left-amygdala_16 Left-amygdala_17 ... Left-amygdala_30	Left amygdala volume at age 5-6 years  Etc..				
hippocampus	Right-hippocampus_1 Right-hippocampus_2 Right-hippocampus_3 Right-hippocampus_4 Right-hippocampus_5 Right-hippocampus_6 Right-hippocampus_7 Right-hippocampus_8 Right-hippocampus_9 Right-hippocampus_10 Right-hippocampus_11 Right-hippocampus_12 Right-hippocampus_13 Right-hippocampus_14 Right-hippocampus_15	Right hippocampus volume at age 0-1 years Right hippocampus volume at age 1-2 years Right hippocampus volume at age 2-3 years Right hippocampus volume at age 3-4 years Right hippocampus volume at age 4-5 years Right hippocampus volume at age 5-6 years  Etc..		mm <sup>3</sup>	Continuous, rounded without decimals	Based on freesurfer v 6.0 output data (aseg file)

	Right-hippocampus_16 Right-hippocampus_17 ... Right-hippocampus_30					
	Left-hippocampus_0 Left-hippocampus_1 Left-hippocampus_2 Left-hippocampus_3 Left-hippocampus_4 Left-hippocampus_5 Left-hippocampus_6 Left-hippocampus_7 Left-hippocampus_8 Left-hippocampus_9 Left-hippocampus_10 Left-hippocampus_11 Left-hippocampus_12 Left-hippocampus_13 Left-hippocampus_14 Left-hippocampus_15 Left-hippocampus_16 Left-hippocampus_17 .... Left-hippocampus_30	Left hippocampus volume at age 0-1 years Left hippocampus volume at age 1-2 years Left hippocampus volume at age 2-3 years Left hippocampus volume at age 3-4 years Left hippocampus volume at age 4-5 years Left hippocampus volume at age 5-6 years  Etc..		mm <sup>3</sup>	Continuous, rounded without decimals	Based on freesurfer v 6.0 output data (aseg file)
Age at neuroimaging	sMRI_age_0 sMRI_age_1 sMRI_age_2 sMRI_age_3 sMRI_age_4	Exact neuroimaging age 0-1 years Exact neuroimaging age 1-2 years Exact neuroimaging age 2-3 years Exact neuroimaging age 3-4 years Exact neuroimaging age 4-5 years		years	Continuous, decimals	



	sMRI_age_5 sMRI_age_6 sMRI_age_7 sMRI_age_8 sMRI_age_9 sMRI_age_10 sMRI_age_11 sMRI_age_12 sMRI_age_13 sMRI_age_14 sMRI_age_15 sMRI_age_16 sMRI_age_17 ... sMRI_age_30	Exact neuroimaging age 5-6 years  Etc..				
--	------------------------------------------------------------------------------------------------------------------------------------------------------------------------------------------------------------------	-----------------------------------------------	--	--	--	--

## Annex IV Example description harmonized variables

- Example: Description of harmonized variables for excel sheets

cohort	domain	dimension	harmonized variable	description	source variables	data type
GenR	Neuroimaging	Structural MRI	etiv_0_5	Estimated intracranial volume at age 0-5 years	TBV_GENR_F@5	continuous

More info on LIFECYCLE online:  
[lifecycle-project.eu](http://lifecycle-project.eu)

interpretation original score	evaluator	number of subjects	Recoding syntax	Software for recoding	Date of harmonization
Number represents volume in mm <sup>3</sup>	MRI machine	2299	<p>***copy new variable with correct name depending on exact age at assessment***.</p> <p>IF (agechild_MRI&lt;12 AND agechild_MRI &gt;=11)            etiv_11=etiv.            VARIABLE LABELS etiv_11            'estimated intracranial volume assessed at between ≥11 year and &lt; 12 years'.</p> <p>*** define level of variable ***.            *** remove decimals ***.</p> <p>VARIABLE LEVEL etiv_11            (SCALE).            FORMATS etiv_11 (f8.0).</p>	IBM SPSS statistics v.25	20/12/2018